Science of the Total Environment 601–602 (2017) 1349–1363

Contents lists available at ScienceDirect

Science of the Total Environment

journal homepage: www.elsevier.com/locate/scitotenv

Central Tibetan Plateau atmospheric trace metals contamination: A 500-year record from the Puruogangri ice core

Emilie Beaudon [a,*], Paolo Gabrielli [a,b], M. Roxana Sierra-Hernández [a], Anna Wegner [a], Lonnie G. Thompson [a,b]

[a] Byrd Polar and Climate Research Center, The Ohio State University, 1090 Carmack Road, Columbus, OH 43210-1002, USA
[b] School of Earth Sciences, 275 Mendenhall Laboratory, The Ohio State University, 125 South Oval Mall, Columbus, OH 43210, USA

HIGHLIGHTS

- Trace metals atmospheric contamination lacks temporal perspective in Tibet.
- 1497–1992 trace elements record extracted from a central Tibetan Plateau ice core.
- Anthropogenic Sb, Cd, Zn, Pb, Ag input begins in 1935 and peaks in 1965.
- Sb, Cd, Zn, Pb reflect Central/South/East Asia metallurgies/coal-burning emissions.
- Monsoon main conveyor of anthropogenic Sb, Pb, Ag to central Tibet since 1980

GRAPHICAL ABSTRACT

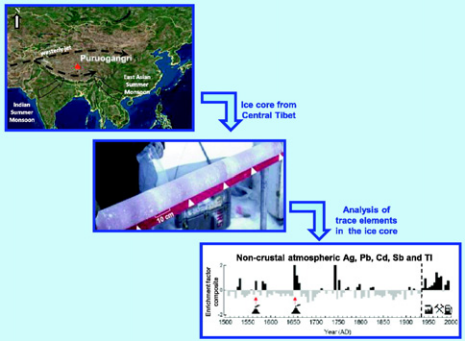

ARTICLE INFO

Article history:
Received 6 April 2017
Received in revised form 16 May 2017
Accepted 21 May 2017
Available online 9 June 2017

Editor: F.M. Tack

Keywords:
Tibet
Ice core
Trace elements
Metallurgy
Westerlies
Monsoon

ABSTRACT

A ~500-year section of ice core (1497–1992) from the Puruogangri ice cap has been analyzed at high resolution for 28 trace elements (TEs: Ag, Al, As, Ba, Bi, Cd, Co, Cr, Cs, Cu, Fe, Ga, Li, Mg, Mn, Na, Nb, Ni, Pb, Rb, Sb, Sn, Sr, Ti, Tl, U, V and Zn) to assess different atmospheric contributions to the ice and provide a temporal perspective on the diverse atmospheric influences over the central Tibetan Plateau (TP). At least two volcanic depositions have significantly impacted the central TP over the past 500 years, possibly originating from the Billy Mitchell (1580, Papua New Guinea) and the Parker Peak (1641, Philippines) eruptions. A decreasing aeolian dust input to the ice cap allowed the detection of an atmospheric pollution signal. The anthropogenic pollution contribution emerges in the record since the early 1900s (for Sb and Cd) and increases substantially after 1935 (for Ag, Zn, Pb, Cd and Sb). The metallurgy (Zn, Pb and steel smelting) emission products (Cd, Zn, Pb and Ag) from the former Soviet Union and especially from central Asia (e.g., Kyrgyzstan, Kazakhstan) likely enhanced the anthropogenic deposition to the Puruogangri ice cap between 1935 and 1980, suggesting that the westerlies served as a conveyor of atmospheric pollution to central Tibet. The impact of this industrial pollution cumulated with that of the hemispheric coal and gasoline combustion which are respectively traced by Sb and Pb enrichment in the ice. The Chinese steel production accompanying the Great Leap Forward (1958–1961) and the Chinese Cultural Revolution (1966–1976) is proposed as a secondary but proximal source of Pb pollution affecting the ice cap between 1958 and 1976. The most recent decade (1980–1992) of the enrichment time series suggests that Puruogangri ice cap recorded the early Sb, Cd, Zn, Pb and Ag pollution originating from developing countries of South (i.e., India) and East (i.e., China) Asia and transported by the summer monsoonal circulation.

Published by Elsevier B.V.

* Corresponding author.
E-mail address: beaudon.1@osu.edu (E. Beaudon).

http://dx.doi.org/10.1016/j.scitotenv.2017.05.195
0048-9697/Published by Elsevier B.V.

1. Introduction

Since the 1980s, Asia has experienced enormous industrial development from rapid population growth, industrialization and consequent large-scale environmental changes. The inherent generated atmospheric pollution currently contributes to half of all Earth's anthropogenic trace metals emissions. Asian trace metal aerosols, when deposited on glaciers of the surrounding mountains of the Himalayan chain and the Tibetan Plateau (TP), leave a characteristic chemical fingerprint (Lee et al., 2008a). These two regions are often referred to as the "Third Pole" due to their climate and considerable volume of glacial ice (Huss and Farinotti, 2012). Despite the importance of the Third Pole region as the primary water source for many of the several billion people living downstream along the great rivers of South and East Asia, the understanding of the environmental change across this vast area and the impact of contaminants is still limited to its margin (e.g., Grigholm et al., 2016), is not properly evaluated (Lee et al., 2008a, 2008b; Xu et al., 2009) or lacks historical perspective (Liu et al., 2011). While the contribution of anthropogenic aerosols to the current weakening of the East Asian Summer Monsoon is vigorously debated (Bollasina et al., 2014; Yang et al., 2016; Yu et al., 2016), the extraction of multi-century atmospheric pollution records from central Tibet is essential to assess the magnitude of the recent contamination of this remote region and to provide a long-term perspective for the changes observed.

Records of past atmospheric deposition preserved in snow and ice from Asian glaciers can offer unique insights into long-term changes of the chemical composition of the atmosphere (Thompson et al., 1989; Kang et al., 2002, 2010; Aizen et al., 2009; Hong et al., 2009; Kaspari et al., 2009a, 2009b; Eichler et al., 2014; Grigholm et al., 2016) and into the nature and intensity of the regional atmospheric circulation systems (Thompson et al., 2000; Eichler et al., 2009; Grigholm et al., 2015). In particular, distribution patterns of the atmospheric contaminants are heterogeneous over the TP (Ramanathan et al., 2007) with zonal, meridional and altitudinal variations induced by the boundaries between continental and marine air masses associated with the dry westerlies and the South Asian monsoon, respectively (Davis et al., 2005; Kaspari et al., 2009b; Tian et al., 2007).

Measurements of windblown aerosol chemical composition and concentrations in ice cores can also yield data to assess the potential contamination of watersheds (Huang et al., 2008), provide geographic constraints to general atmospheric circulation models (Gao et al., 2016) and help identify sources of anthropogenic aerosols affecting the atmospheric radiative forcing. These impact assessments may subsequently inform decisions on emission controls to mitigate climate change (Streets et al., 2013).

Earlier studies from Mt. Everest (Kang et al., 2007; Lee et al., 2008a, 2008b; Hong et al., 2009; Kaspari et al., 2009a, 2009b; Zhang et al., 2009) revealed that even the highest and most remote glaciers of this region are affected by trace metals pollution originating from anthropogenic sources (i.e., coal and oil combustion, non-ferrous metal production) and through "brown clouds" transported during the pre-monsoon season (Reddy et al., 2005; Gustafsson et al., 2009; Bonasoni et al., 2010; Lüthi et al., 2015). Interpreting trace element (TE) records from glaciers implies a thorough comprehension of their provenance and temporal variability. It is then essential to discriminate the TEs' natural background components (e.g., terrestrial or volcanic constituents) from their anthropogenic components (Gabrielli et al., 2008). This specific task is rather complex for TP ice cores because volcanic and anthropogenic contributions are overwhelmed by local, terrestrially-derived aerosol fallout of crustal origin (Li et al., 2009).

The ice core collected from Puruogangri glacier in 2000 contains an extended reconstruction of central TP atmospheric pollution. The Puruogangri ice cap (33°55′N, 89°05′E, 6072 m a.s.l.) lies in the western Tanggula mountain range where seasonal melting of its snow and ice feeds the large surrounding lakes such as Linggo Lake (Pan et al., 2012; Xu et al., 2009) and Dogai Coring Lake (Yan and Zheng, 2015). Puruogangri is of particular climatological interest because of its location in the transition zone between the monsoon-dominated south and the dry, westerly-dominated north (Fig. 1) (Tian et al., 2007; Thompson et al., 2006; Yao et al., 2012, 2013). The pressure gradient between southwestern Asia (low pressure) and the Indian Ocean (high pressure) drives the South Asian Summer Monsoon, the principal moisture contributor to the TP in the warmest months from June through September (Yanai et al., 1992; Webster et al., 1998, Tian et al., 2007; You et al., 2008; Joswiak et al., 2013; Maussion et al., 2013). Limited winter precipitation results from the dry, continental westerlies, which also act as a potential dust carrier to the ice cap. The first Puruogangri glaciochemical measurements (Thompson et al., 2006) revealed the connection between drought events and weakening of the monsoon system (Davis et al., 2005; Yang et al., 2014). The enriched $\delta^{18}O$ events in the Puruogangri ice core in the late 1920s and around 1990 induced by long distance moisture transport showed that the area has been affected by warming and intensified moisture conditions in the 20th century (An et al., 2016).

This study presents a 500-year atmospheric contamination history which, along with the Geladaindong Hg record (Kang et al., 2016), is the oldest (to date) trace and ultra-trace elements concentration record for the central TP. Here the TE record is used to characterize the natural (i.e., deserts, lakes and volcanoes) and anthropic sources of atmospheric aerosols preserved in the Puruogangri ice. Particular attention is given to assessing TEs originating from anthropogenic sources during the 20th century that relies on a subtle discrimination between the anthropogenic contribution and the crustal background. The Puruogangri ice core atmospheric pollution histories are compared with records from the TP region (Kang et al., 2007; Lee et al., 2008a, 2008b; Hong et al., 2009; Grigholm et al., 2016), the Siberian Altai (Eichler et al., 2012, 2014) and Greenland (McConnell and Edwards, 2008) taken as a hemispheric reference. These Puruogangri TE records provide new evidence of the dynamic and depositional characteristics of aerosol pollutants during the last 500 years.

2. Materials and methods

2.1. The Puruogangri ice core

Three deep ice cores from the Puruogangri ice cap were recovered in 2000 in a collaborative effort between the Laboratory of Ice Core and Cold Regions Environment (LICCRE) of the Cold and Arid Regions Environmental and Engineering Research Institute (CAREERI) and the Byrd Polar and Climate Research Center (BPCRC). The state of the firn archive prevented any consistent sampling of the top 3 m of the core. Consequently, the 1992–2000 period is excluded from our study. This paper presents the TEs records obtained from 3 m (corresponding to an age of 1992 CE) down to 123.7 m (corresponding to an age of 1497 CE) of the longest core (C2, 214.7 m long) which was drilled on Dome A (5980 m a.s.l.) of the ice cap (Thompson et al., 2006). Ice temperatures were −6 °C at 10 m and −0.9 °C at the bottom of the borehole, which did not reach bedrock. The distinct annual dust layers and the chemical analysis for stable water isotopes, β radioactivity, major ions and insoluble particles allowed the development of an annually-resolved time scale back to 1600 CE. The β horizon peak from the 1963 atmospheric nuclear bomb tests was measured at 14.5 m depth giving an average accumulation rate of 0.38 m ice equivalent per year. The dating uncertainty increases with depth: from ±1 yr above the 1963 horizon to ±15 yrs. at 1600 (107.6 m depth) (Thompson et al., 2006).

2.2. Ice core sampling and chemical analysis

Sample sizes ranged from 3 to 10 cm depending on the depth of the ice processed and on the sample temporal resolution targeted. The samples were continuously cut with a carbon steel band saw from the inner part of the core along 3–123 m interval of the core spanning the time

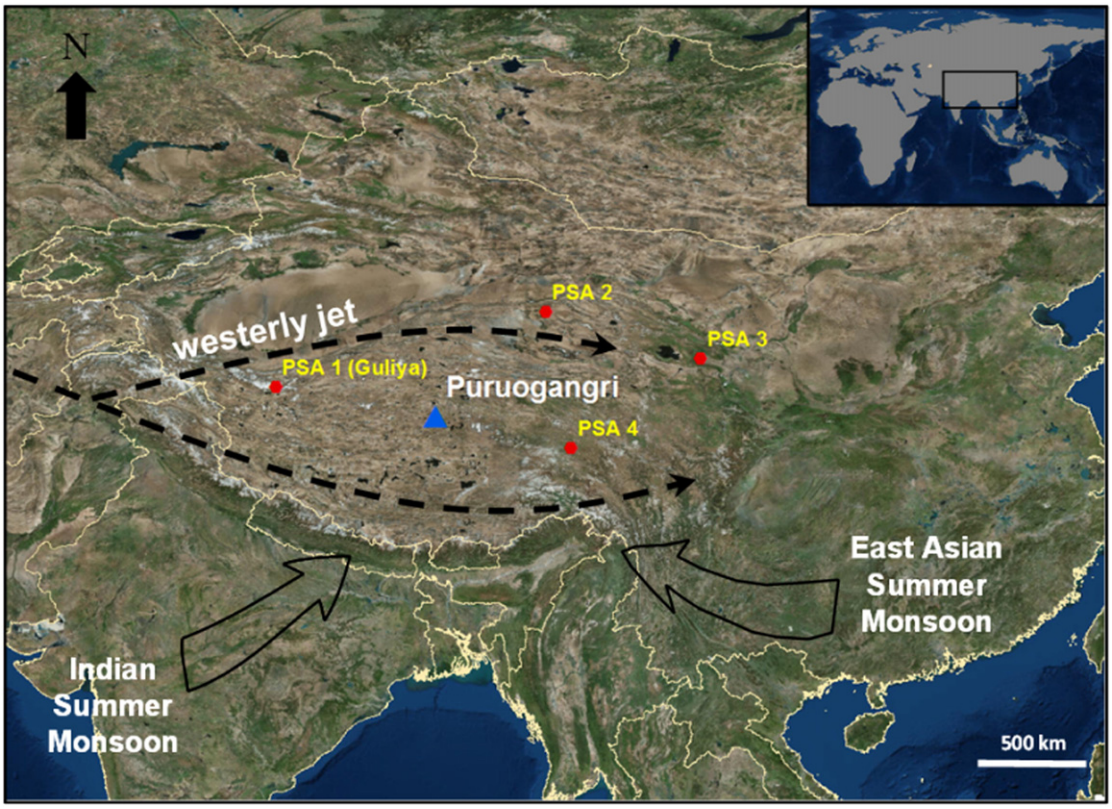

Fig. 1. Map of the "Third Pole region" showing the ice core site (blue triangle) and the dust sampling sites (Potential Source Areas of dust (PSA), red dots). Mid-latitude westerlies are deflected by the elevated topography of the Tibetan Plateau and split into a northern and a southern branch.
Source: Background image: ESRI, world imagery.

period from the year 1497 to 1992. The sampling resolution ranges between 2 and 8 samples per year at 1497 and 1992, respectively. The sample preparation was conducted in a class 100 clean room. A total of 1791 samples were decontaminated by triple washing with ultrapure water before they were melted at room temperature into pre-cleaned low-density polyethylene (LDPE) bottles and transferred into acid cleaned LDPE vials. These aliquots were then acidified with ultra-pure HNO_3 (Optima grade) to a final concentration of 2% (vol/vol) and set aside for 30 days to allow TE leaching (Uglietti et al., 2014). Subsequently, samples were stored in a freezer or analyzed for TEs by Inductively Coupled Plasma Sector Field Mass Spectrometry (ICP-SFMS; Element2, Thermo Scientific). Uglietti et al. (2014, 2015) and Gabrielli et al. (2014) describe in detail the analytical method employed here for their analysis of 18 TEs. Ten additional TEs (Ba, Cs, Ga, Li, Mg, Na, Nb, Ni, Sn and Sr) have been analyzed in the framework of this study and their limit of detection, procedural blank, precision and accuracy results are summarized in Table A. The mean procedural blank values were lower than the minimum concentrations determined in the ice core. Thus, the procedural blanks were negligible in the calculation of TE concentrations in the Puruogangri samples. The instrumental detection limits, calculated as three times the standard deviation of 10 measurements of ultrapure water, ranged from 0.01 $pg \cdot g^{-1}$ for Tl to 0.2 $ng \cdot g^{-1}$ for Na (Table A). When compared to the detection limit, the minimum concentration measured in Puruogangri ice samples was 37 times greater for Tl and 119 times greater for Na. A certified material solution (TM Rain 95, Environment Canada) was diluted ~20 times and was systematically analyzed at the beginning of each analytical session to assess the accuracy of the method. Good agreement between measured and certified values was found for all elements (accuracy within 4–18%) except for Li, which has an accuracy of 30%. The overall precision was estimated as the deviation from the mean of 22 replicate measurements of the certified material during a three-month period. The precision ranged from 2% for Bi, Fe, Mn, Sn and Zn to 19% for Ti and 49% for Ga.

2.3. Enrichment factor

The crustal Enrichment Factor (EF) was used as a diagnostic tool to differentiate the non-crustal contribution from the crustal background. It is defined as the ratio of the concentration in the ice of a given element to that of an element assumed to be representative of rock and soil, normalized to the same ratio obtained from a crustal reference (Zoller et al., 1974; Duce et al., 1975; Gabrielli et al., 2005; Kaspari et al., 2009b; Krachler et al., 2009; Cong et al., 2015). As Fe is rather stable and abundant in rock and soil dust (6%; Wedepohl, 1995), precisely and accurately determined by ICP-SFMS and highly correlated to Al concentration ($r = 0.99$ in our samples), Fe was used as the conservative crustal element of reference (Uglietti et al., 2015).

$$EF = \{[TE]/[Fe]\}_{ice} / \{[TE]/[Fe]\}_{TP}$$

where: $\{[TE]/[Fe]\}_{ice}$ and $\{[TE]/[Fe]\}_{TP}$ are respectively the mass ratio between a given TE and Fe in the ice sample, and in Tibetan Plateau dust samples from Potential Source Areas (PSA) of aeolian dust. Here the PSA samples consist of the aeolian fraction of soil dust samples collected by the Ice Core and Paleoclimatology Group of the BPCRC in various regions of the TP and assumed to constitute a regional pool of crustal reference samples (Fig. 1). Normalizing $\{[TE]/[Fe]\}_{ice}$ to a regional TP crustal reference (i.e., PSA samples from TP) has two advantages compared to the commonly used Upper Continental Crust (UCC) reference (Wedepohl, 1995):

I. The same chemical leaching procedure (in this study: a simple acidification) is employed for the preparation of the Puruogangri ice

samples and for the PSA dust samples. This nullifies the analytical bias linked to differential mass fraction recovered by acid leaching and grinding and fusion processing used to analyze geological samples (by X-ray spectrography) and to calculate the UCC concentrations (Norrish and Hutton, 1969; Shaw, 1960; Shaw et al., 1967; Wedepohl, 1995).

II. Due to geological variability, the ratio of crustal elements in atmospheric particles can differ significantly from the UCC crustal ratio. For instance, As has much higher concentrations in TP soils relative to UCC average crustal values (EF > 10) (Li et al., 2009) which would result in EF values of As in ice samples above the conventional threshold of 10 (i.e., EF > 10) and thereby be attributed erroneously to a non-crustal contribution. Establishing a local crustal reference can greatly reduce this effect and account for the natural enrichment of some specific elements in the Tibetan soils, with the assumption that the PSA dust samples are pollution free (Erel et al., 2006). Using the PSAs as a reference then provides smaller EF absolute values than with the UCC reference (e.g., the pre-1900 median Sb $EF_{UCC} = 6.7$ while the pre-1900 median Sb $EF_{TP} = 1.8$ (Table 1)) (Marx et al., 2008; Uglietti et al., 2015). Thus, this method allows the evaluation of much smaller variations of the EF.

Differences in transport behavior between the TE of interest and the TE of reference (i.e., Fe) is another factor that can affect the absolute value of EF (Krachler et al., 2005; Marx et al., 2016). The very high dust (and Fe) concentrations in the Puruogangri ice (Section 3.1.) also greatly contribute to reducing the EF absolute values.

In this study, the distinction between the crustal and non-crustal origin of the various TEs is not based on an arbitrary EF threshold but rather on amplitudes and trends of EF excursions from the EF median calculated over the pre-industrial period (i.e., 1492–1900) encompassed by this ice core record. The significance of these excursions from the median is assessed by applying the Mann-Whitney test on the increase factor (IF) calculation (Table 1).

Table 1
Statistical data for elemental concentrations and enrichment factors (EFs). Increase factors (IF) between the 1497–1900 and the 1900–1992 periods are in bold type if significant at the 95% level (Mann-Whitney test).

	1497–1992				Pre-1900		Post-1900		IF	IF
	Min	Max	Median		Median		Median		(Conc.)	(EF)
	pg·g^{-1}	pg·g^{-1}	pg·g^{-1}	EF	pg·g^{-1}	EF	pg·g^{-1}	EF		
Ag	0.147	93	2.3	2.3	2.2	2.2	2.5	2.9	1.1	**1.3**
As	28	7300	410	1.7	420	1.7	370	1.7	0.9	1
Bi	0.23	440	6.3	1.4	6.6	1.3	5.9	1.5	0.9	**1.1**
Cd	0.80	540	8.5	2.7	8	2.4	9	3.4	**1.2**	**1.4**
Co	7.8	5800	192	1.1	195	1.1	179	1.1	0.9	**1.1**
Cr	16.1	13,700	460	1.1	480	1.1	440	1.1	0.9	1
Cs	10.82	5800	232	1.9	243	1.9	203	1.8	0.8	1
Cu	48	12,600	520	1	540	1	480	1.1	0.9	**1.1**
Ga	3.6	2350	82	0.9	85	0.9	71	0.9	0.8	1
Li	170	18,500	1350	2	1430	2.1	1110	1.8	0.8	0.8
Nb	1.20	250	22	1.1	24	1.1	17	1	0.7	0.9
Ni	26	16,900	550	1.2	570	1.2	510	1.2	0.9	1
Pb	30	81,000	780	1.9	770	1.8	810	2.3	1	**1.3**
Rb	45.2	18,000	730	1.1	790	1.1	630	1	0.8	0.9
Sb	1.24	1900	24	2	23	1.8	27	2.5	**1.2**	**1.4**
Sn	2	130	9.7	1.6	9.6	1.5	9.9	1.7	1	**1.1**
Tl	0.37	420	7.5	1.6	7.5	1.5	7.5	1.7	1	**1.1**
U	2.32	580	44	0.9	50	0.9	36	0.8	0.7	0.9
V	19.1	13,500	470	1.1	490	1.1	413	1.1	0.8	1
Zn	75	77,000	1490	1.6	1490	1.6	1473	1.8	1	**1.2**
	ng·g^{-1}	ng·g^{-1}	ng·g^{-1}	EF	ng·g^{-1}	EF	ng·g^{-1}	EF		
Al	11.7	7200	267	1	282	0.9	239	1	0.8	1
Ba	0.18	173	5	1.6	5.2	1.6	4.8	1.7	0.9	**1.1**
Fe	11.7	11,400	348	1	364	1	315	1	0.9	1
Mg	23.8	8200	352	1.1	362	1.1	315	1.2	0.9	1
Mn	0.65	700	15	1.5	15.3	1.5	14.8	1.7	1	**1.2**
Na	23.4	4400	478	1.1	533	1.2	371	1	0.7	0.8
Sr	0.5	370	11	1.2	11.8	1.3	8.3	1.1	0.7	0.9
Ti	0.8	500	19	1.2	20.5	1.2	17.5	1.1	0.9	0.9

3. Results and discussion

Statistical properties of TE concentrations and EFs are presented in Table 1 and Fig. A1. In addition to the 500-year median values, Table 1 displays TE median concentration for the pre-1900 and post-1900 periods. The pre-1900 period is chosen as the background reference and will be used throughout this paper as it has been used in other studies (Kaspari et al., 2009b; Grigholm et al., 2015) because anthropogenic inputs in Asia are expected to be negligible before 1900.

3.1. Influence of the surrounding deserts

A vast desert of carbonaceous sandy hills surrounds the Puruogangri ice cap over a minimum perimeter of 2000 km (Fig. 2; Kreutz and Sholkovitz, 2000; Han et al., 2009; Yang et al., 2015). In this area, there are fewer lakes than in the southern TP but their salinity is greater along a SE-NW salinity gradient driven by the summer monsoon extent (Yan and Zheng, 2015). Due to this arid surrounding environment, the low snow accumulation (0.38 mwe·y^{-1}) and the inherently large dust content of the Puruogangri ice (1497–1992 median dust concentration = 175 μg·g^{-1}), the elemental concentrations rank among the highest measured across the Third Pole region. However, caution is required when comparing several ice core-derived TE concentrations as different leaching procedures have been employed in other ice core studies which could account for some of the difference observed in the concentration ranges (Uglietti et al., 2014).

Na, Mg, Fe and Al concentrations are the most abundant TEs in Puruogangri with respective medians of 478 ng·g^{-1}, 352 ng·g^{-1}, 348 ng·g^{-1} and 267 ng·g^{-1}. Ti, Mn, Sr, Ba, Zn and Li were also determined at the ng·g^{-1} level (Fig. A). The other 18 elements analyzed in the ice were all below the ng·g^{-1} level with the smallest concentrations obtained for Ag (min [Ag] = 0.147 pg·g^{-1}, Table 1).

Fig. 3 displays the median of the EFs of the TP PSA samples using the UCC as a reference (Wedepohl, 1995). Our results are in agreement with those of Li et al. (2009), indicating the characteristic enrichment of TP soils (Currell et al., 2011; Zhang, 2014) in As (10.8) and Cs (2) and also in Li (2.4), Cd (3.1) and Bi (3.3). The Sb enrichment (3.7) of the TP dust results from surface soil samples collected near the Guliya ice cap (Western Kunlun Shan) where Sb is naturally enriched (Hou and Cook, 2009). The high Li content of the PSA dust samples reflects the chemical composition of numerous TP lakes, some of them dried out (paleolakes), containing extremely high concentrations of Li salts (Fan et al., 2010; Hudson and Quade, 2013; Lafitte, 2013). The substantial amount of evaporitic deposits across the TP could also explain the slight enrichment in the TP PSA samples in Mg, Mn, and Sr (Williams et al., 2004; Yang et al., 2015).

The bulk elemental enrichments of the pre-1900 Puruogangri ice relative to the UCC reference matches that of the TP PSA. When the bulk pre-1900 Puruogangri EF in ice is calculated using the TP dust mass ratios from the PSA as a crustal reference, no significant enrichment is observed for any of the 28 TEs. This illustrates that the pre-industrial elemental budget was dominated by regional dust, which is well represented by our PSA dust samples.

3.1.1. Multivariate analysis of TE concentrations

To extract shared variance between elements and to discriminate the sources contributing to the elemental concentration budget, an Empirical Orthogonal Function (EOF) analysis was performed on the 28 TEs high resolution time series of log-transformed concentrations for the 1497–1992 period. The measurement uncertainty being around 3%, no >97% of the variance can be expected to be physically explainable. The leading four EOFs were significant (significance testing against white

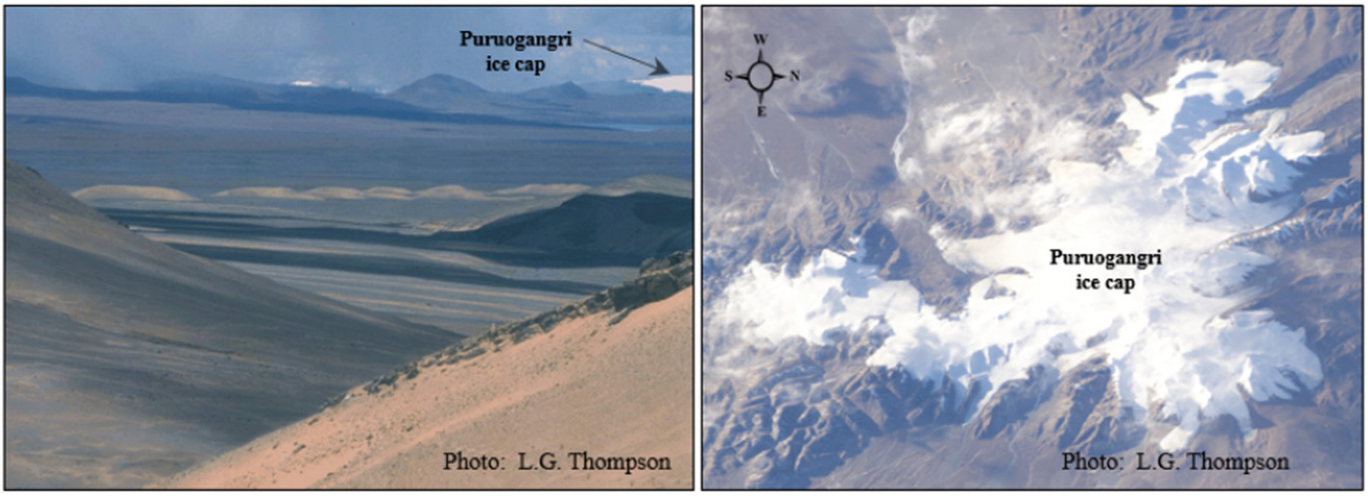

Fig. 2. Sand dunes surrounding Puruogangri ice cap (left) and aerial view of the Puruogangri ice field (right).

noise (Moore and Grinsted, 2009)) and account for 95% of the variance. Table 2 displays only the three leading eigenvectors, which together account for 93.2% of the variance.

The first eigenvector (EOF 1) describes 82.2% of variance in the dataset. EOF 1 is loaded in Fe and almost all other elements except Na and Sr, which have the lowest loading coefficients (0.06 and 0.11 respectively). This indicates that the concentration variance is largely influenced by the crustal dust input.

EOF 2 accounts for 8.4% of the variance and is mainly loaded in Na, Sr, U, Li, Ti and to a lesser extent in As and Mg (the former is significantly enriched in TP dust, Fig. 3). This association possibly reflects the higher water solubility of these specific elements (Dean, 1987, 2013) compared to the other 22 elements in this study. Hence, the EOF 2 signal could represent a contribution from the evaporite deposits (halite, gypsum) surrounding the Puruogangri ice cap (Fig. 2; Zhang et al., 2001; Cong et al., 2007; Zheng and Liu, 2009) and/or in part, originating from the vast desert regions of Central Asia (e.g., in Kazakhstan (Indoitu et al., 2012)) and the Middle East (e.g., Saudi Arabia (Prakash et al., 2016)). The EOF 1 and 2 time series are plotted in Fig. B and give an indication of the temporal variations of the lithogenic and the evaporitic contribution to the Puruogangri ice TE budget. EOF 2, representing the evaporitic component of the total dust, decreases from 1900 and throughout the 20th century. This trend mirrors that of the concentrations of ionic constituents (Cl^- for instance, Fig. B) of salts derived from nearby lake beds (Thompson et al., 2006). For the same period, Chu et al. (2008) and Yao et al. (2008) reported an increase in the snow accumulation rate on Puruogangri, which may have induced dilution and the decreasing concentration of soluble species.

About 2.6% of the variability of the Puruogangri chemical dataset is due to the elements loaded in EOF 3: Ag, Ba, Cd, Pb, Tl and especially Sb, while none of the main dust-derived elements (i.e., Fe, Mg, As) are significantly loaded. This suggests that EOF 3 (Fig. B) represents a non-crustal source such as quiescently degassing volcanism (Lambert et al., 1988; Hinkley et al., 1999) or an anthropic source. These heavy metals, except Ba, respectively show a 7, 5, 7, 4 and 3-fold increase in concentration (between 1945 and 1990) with respect to pre-1900 that is in contrast with the decreasing trend of the total dust concentration (Fig. B). This implies that a non-crustal contribution has occurred in the heavy metals budget.

With the exception of Ba, the concentration of the TEs loaded in EOF 3 (Ag, Cd, Pb, Sb and Tl) increases during the 20th century (Table 1). This is fairly well reflected by the composite time series (EF*) of 5-year EF median of these five TEs (Ag, Cd, Pb, Sb and Tl, Fig. B). In addition, the EF of Ag, Cd, Pb, Sb and of Zn all increase significantly, by 20% or more, during the 20th century (Table 1 and Section 3.3.). Thus, the discussion thereafter focuses on these four TEs (Ag, Zn, Pb, Cd and Sb).

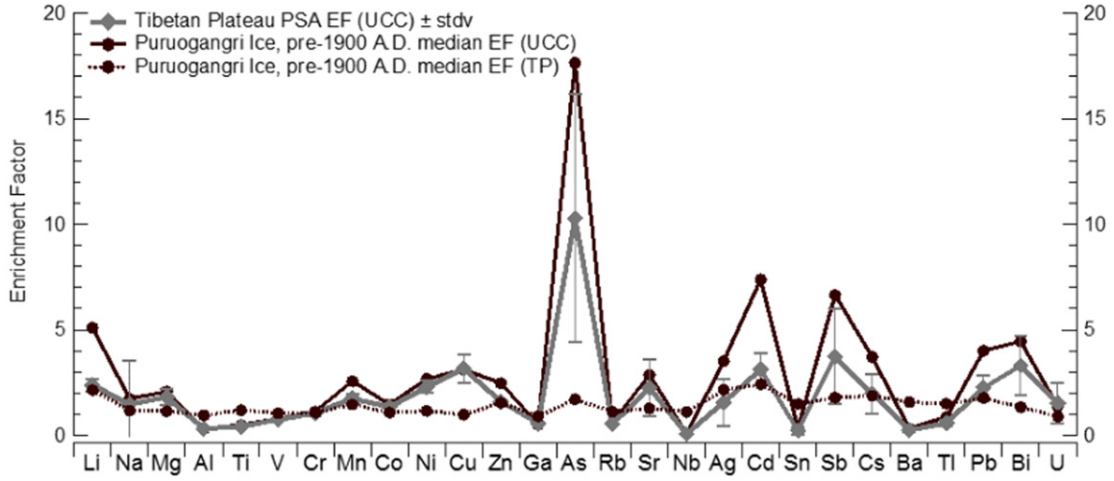

Fig. 3. Average EFs of TP PSA dust samples (grey) relative to the Upper Continental Crust (UCC). The vertical bars represent the variability (standard deviation) between the 4 Potential Source Areas (PSA) of dust sites. Fe is the crustal element of reference. For comparison, the Puruogangri ice core pre-1900 CE median of the EF relative to UCC (solid line) and relative to TP PSA (dash line) are also presented.

Table 2
Loading coefficients of 28 TEs obtained by EOF analysis of the high-resolution, log-transformed concentration records for the period 1497–1992. Bold numbers represent the 95% significance.

TE	EOF 1	EOF 2	EOF 3
Ag	**0.19**	0.08	**−0.29**
Al	**0.20**	0.12	0.16
As	**0.19**	−0.14	0.01
Ba	**0.19**	−0.11	**−0.24**
Bi	**0.20**	0.10	−0.02
Cd	**0.19**	0.07	**−0.34**
Co	**0.20**	0.12	0.13
Cr	**0.20**	0.12	0.19
Cs	**0.20**	0.07	0.00
Cu	**0.20**	0.05	0.09
Fe	**0.20**	0.12	0.15
Ga	**0.20**	0.12	0.18
Li	**0.19**	**−0.21**	0.10
Mg	**0.20**	−0.12	0.12
Mn	**0.20**	0.09	−0.07
Na	0.06	**−0.56**	0.22
Nb	**0.19**	0.09	0.27
Ni	**0.20**	0.11	0.13
Pb	**0.19**	0.09	**−0.35**
Rb	**0.20**	0.04	0.07
Sb	**0.18**	−0.05	**−0.42**
Sn	**0.17**	−0.06	0.19
Sr	0.11	**−0.51**	−0.10
Ti	**0.18**	**−0.24**	−0.03
Tl	**0.20**	0.01	**-0.21**
U	**0.17**	**-0.34**	0.02
V	**0.20**	0.09	0.18
Zn	**0.20**	0.12	−0.04
Variance (%)	82.2	8.4	2.6
Cum. variance (%)	82.2	90.6	93.2

3.1.2. Ag, Zn, Pb, Cd and Sb concentration time series

The 5-year medians of Ag, Zn, Pb, Cd and Sb concentrations over the past 500 years are illustrated in Fig. 4. Ag, Zn, Pb, Cd and Sb concentration time series coincide with the dust record (respectively $r = 0.46$, 0.57, 0.48, 0.55 and 0.41, $p < 0.005$) and show no clear trend over the past 500 years. Yet, all TE concentration 5-year medians (Table 1) are between 2 and 43% higher during the pre-1900 period except for Ag, Cd and Sb. The most remarkable feature in the 500-year TE concentration records is the large peak spanning ~40 years and centered around 1810, which corresponds to the driest period at the end of the Little Ice Age (LIA) in Tibet (between 1780 and 1830 according to Yao et al., 1997; Thompson et al., 2006). Central TP was at that time more influenced by the North Atlantic Oscillation (NAO) and by the baroclinity between Eurasia and Asia rather than by the tropical monsoons (Davis et al., 2005; Zhang et al., 2015). In this atmospheric context, westerly circulation was enhanced and the dust input to the ice cap was higher.

Different peaks in Ag, Zn, Pb, Cd and Sb (and As, Bi and Tl (not shown)) are observed in the annual average concentration records (Fig. 4) and could be attributed to short-term events. Considering the high crustal dust background, only detailed examination of the EF records can yield a robust conclusion regarding the attribution of the source (volcanic, see Section 3.2.2.).

3.2. Non-crustal sources during the 1497–1900 period

Emergence of TE enrichment could be the result of: i) the activation of an anthropic source of emission, ii) a change in wind circulation or iii) a change in the snow deposition mode and post-depositional processes. Visual stratigraphic inspection (clear ice layers) and previous glaciochemical investigations of the Puruogangri core (Thompson et al., 2006; Yao et al., 2008) indicate that the annual melt does not exceed 10% in the upper part of the core which is not sufficient to compromise the TE distribution within annual snow layers (Wong et al., 2013). In an ice core record overwhelmed by the crustal input, fourth possibility could be that a transient lower crustal dust input has allowed detection of a non-crustal signal that is either anthropogenic or volcanic.

3.2.1. Possible medieval anthropic sources of atmospheric pollution

The contribution of non-crustal sources to the Puruogangri Ag, Zn, Pb, Cd and Sb budget is illustrated by their EF time series (Fig. 5a, EF* in Fig. B). Besides the enrichment induced by volcanic fallouts (Section 3.2.2.), EF values sporadically exceed the 1492–1900 median during the 16th century and the 18th century for Sb and especially for Ag, Pb

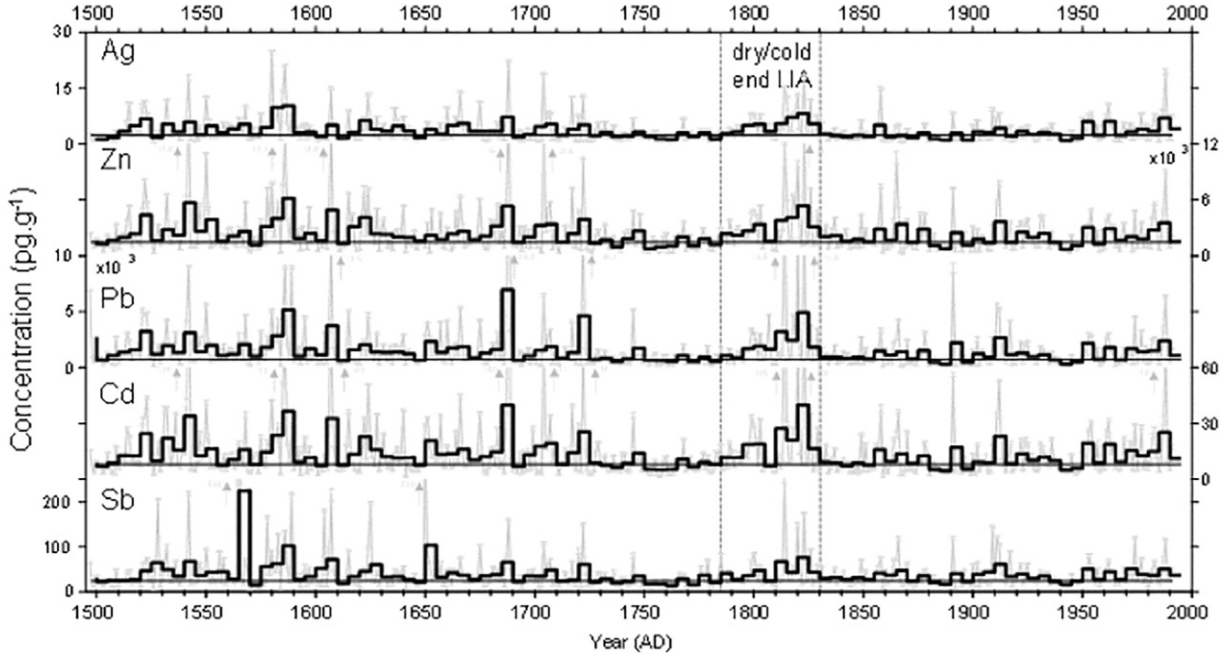

Fig. 4. Annual median (grey line) and 5-year average (step plot) concentration time series of Ag, Zn, Pb, Cd and Sb. The horizontal lines are the medians over the pre-1900 period. The vertical dashed lines frame the termination of the LIA in Tibet (Thompson et al., 2006).

and Cd. These enrichments indeed occur at times of lesser crustal input (Fig. B). During the 16th century, Pb and Ag enrichment occurs and EF values are as high as those of the post-1900 industrial period (Pb EF ~ 4, Ag EF ~ 3.5). Cd is also enriched during the 18th century (Cd EF ≥ 3). An anthropogenic origin of Pb, Ag, Sb and Cd is possible considering the well-known metallurgical developments, especially in the Yunnan province (bordering Tibet on the southeast, Fig. 6), during the Ming (1368–1644) and the Qing (1644–1911) dynasties (Yang, 2004; Lee et al., 2008a, 2008b; Hillman et al., 2014, 2015). Furthermore, atmospheric Zn and Cd contamination of Puruogangri ice could have come from ancient smelting activities in Rajasthan (India) and Taxila (now Pakistan), where Zn and brass (a zinc alloy) were produced on an industrial scale during the Middle Ages (Hegde, 1989; Craddock et al., 2010, Marx et al., 2016). These two regions are located within the highest air mass trajectory frequencies reaching central Tibet (see Section 3.3.) and thus, the Puruogangri ice cap.

Part of the contamination of the Puruogangri ice may have also resulted from biomass combustion across the TP where the traditional pastoral economy and livelihood has relied on yak dung combustion since pre-historical times (Rhode et al., 2007; Bauer, 2006) until the present time (Zhou et al., 2017). Chen et al. (2015) demonstrated the relationship between yak dung combustion and the heavy metal (mostly in Pb, Cd and Zn in their study) contamination of snow in southern Tibet (Nam Co region). Although further investigation is required to explain an intermittent contamination signal in the ice, yak dung burning could be counted as a minor but plausible local contributor to the enrichment of atmospheric heavy metals in the Puruogangri core during the pre-industrial period.

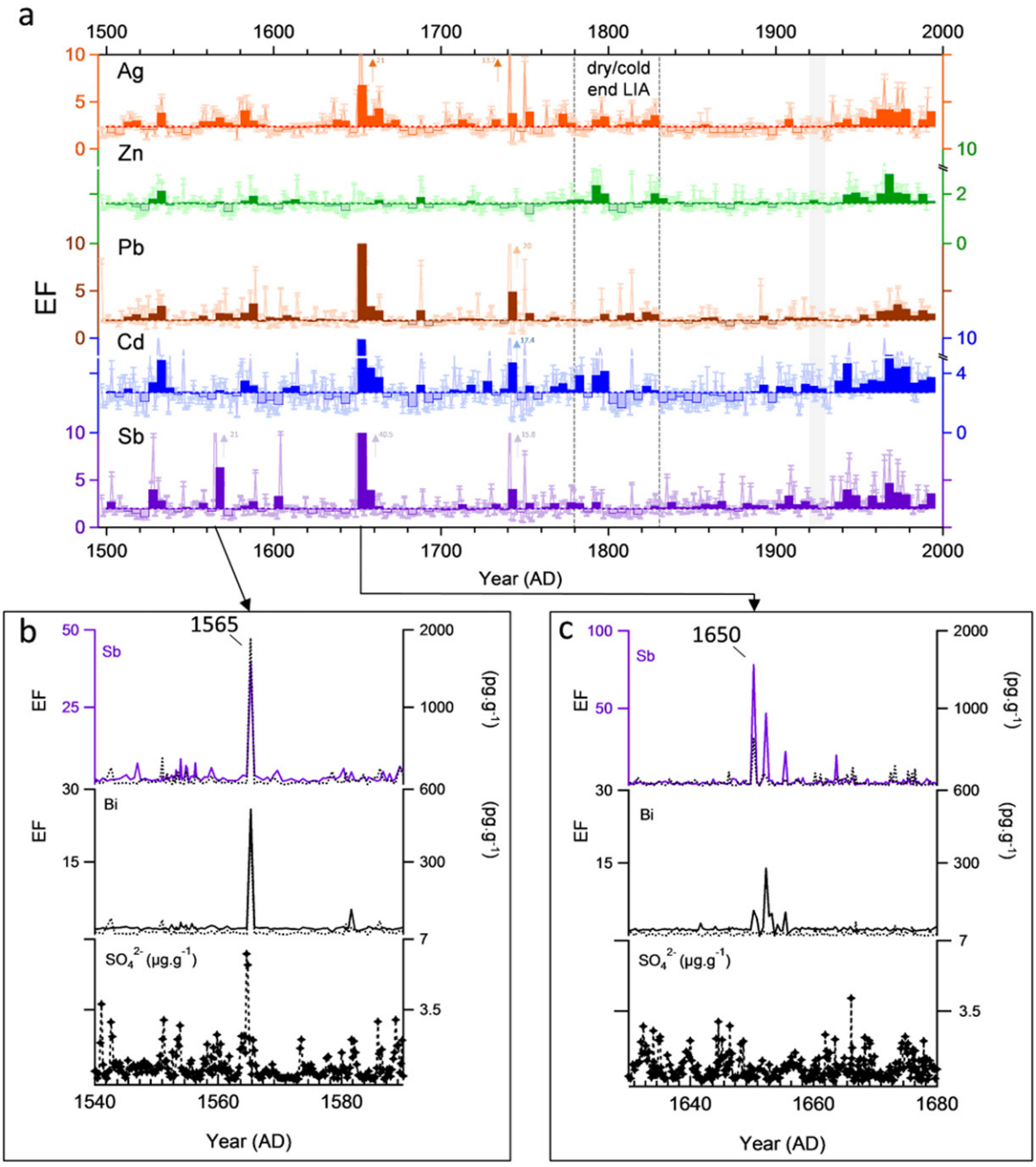

Fig. 5. a) 5-year average enrichment factor (EF) time series (bar plot) of Ag, Zn, Pb, Cd and Sb. The horizontal lines are the medians over the pre-1900 period. The vertical dashed lines frame the termination of the LIA in Tibet (Thompson et al., 2006). The grey area marks the wet and warm 1920s (Thompson et al., 2006). Possible volcanic horizons at b) 1565 (Billy Mitchell (1580)) and c) 1650 (Parker Peak (1641) with high resolution EF time series for Sb, Bi (dotted lines represent the concentration) and SO_4^{2-} (dashed line).

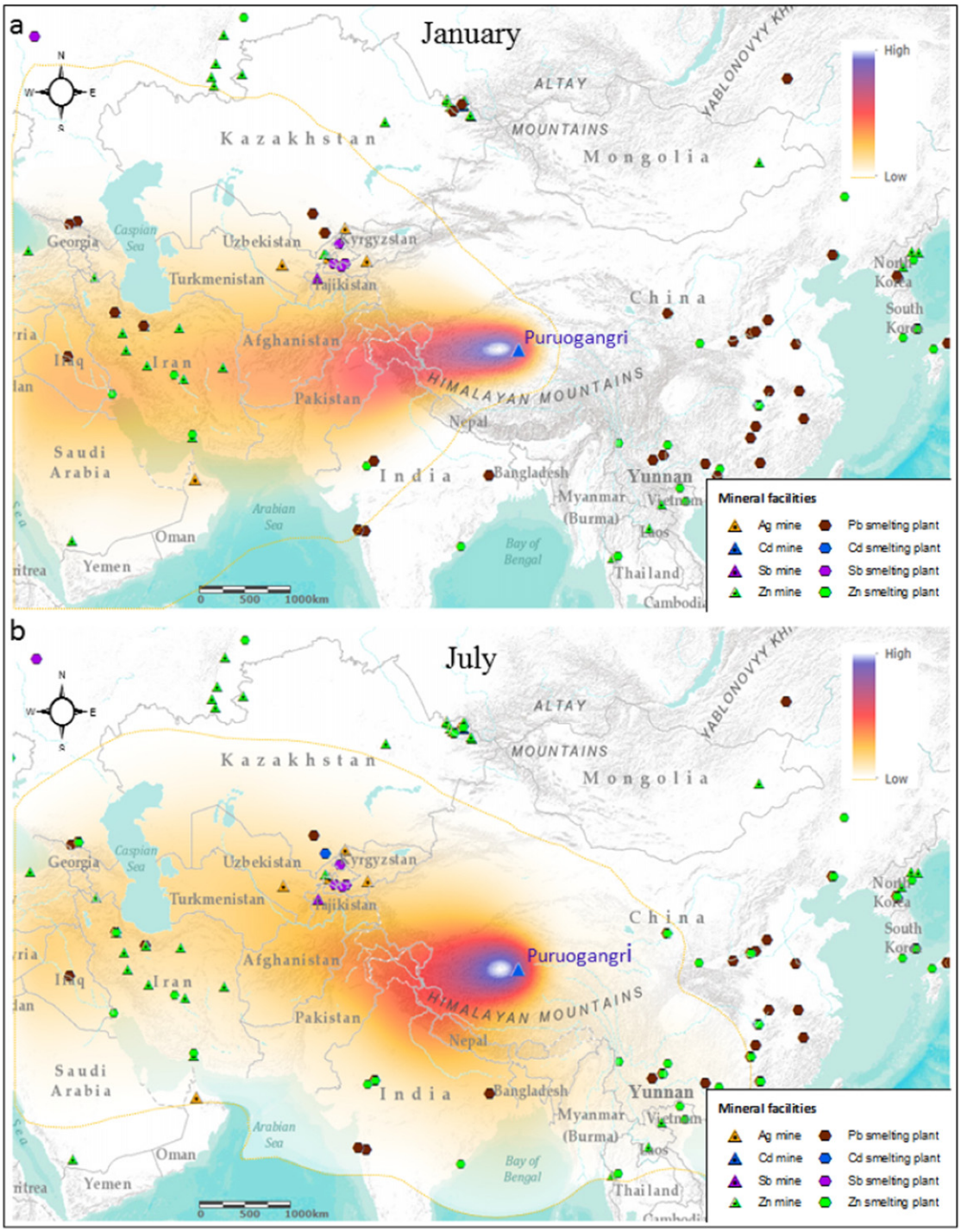

Fig. 6. Mine (triangles) and smelting plant (hexagons) locations for Ag (orange), Cd (blue), Pb (brown) and Sb (purple) (Baker et al., 2010). Back trajectories frequencies are represented by colored area with high frequencies in white and blue to lower frequencies in yellow. The NOAA HYSPLIT (Stein et al., 2015) 7-day back trajectories have been computed for every day of January (middle of the dry season) as shown in a) and of July (middle of the wet season) as shown in b), using NCEP Reanalysis 1 for the 1948–1992 period.

3.2.2. Volcanic contribution

Intermittent and moderate enrichment in Ag, Zn, Pb, Cd and Sb during the 16th and 18th centuries may as well reflect the emissions from volcano vents or geothermal fields present in tectonically active areas of Tibet (Guo and Wang, 2009; Guo et al., 2009; Guo, 2012). On the other hand, the highest peaks in EF characterize distant explosive volcanic eruptions.

Bi is considered as a tracer of volcanic emissions (Lambert et al., 1988; Le Cloarec et al., 1992) and has been used to extract records of past explosive volcanic activity from ice cores (Ferrari et al., 2001; Kaspari et al., 2009b). Considering that fallout materials from erupting volcanoes are enriched in Sb, Cd, Zn and Pb (Nho et al., 1996), EF peaks in these TEs in the Puruogangri record could indicate volcanic horizons.

Peak concentration and enrichment in 1565 in Sb (EF = 39) and Bi (EF = 26) are likely the trace of an explosive volcanic eruption perhaps attributed to the Billy Mitchell volcano (Papua New Guinea) in 1580 (±20 years) (Fig. 5b). A large sulfate spike (6.2 $mg \cdot g^{-1}$) is also measured in Puruogangri in the 1565 horizon (113.1 m depth) which occurs in a relatively less dusty section of the core (Fig. B).

The 5-year averaged EFs of Ag, Pb, Cd and Sb exceed the value of 7 for a prominent peak around 1650. This peak is conspicuous in the high resolution records of Sb EF and concentration and of Bi EF (Fig. 5c). Considering the dating uncertainty at this depth (±15 years at 1600 CE), this layer (96.7 m depth) could be associated with the 1641 Parker Peak eruption (stratovolcano, Philippines). Interestingly, the 1641 Parker Peak volcanic peak was also detected in the sulfate record from the Everest ice core (Kaspari et al., 2009a; Moore et al., 2012).

3.3. 20th century anthropogenic contamination and potential sources

In a TE record dominated by the lithogenic contribution, an anthropogenic signal could be detected as a result of decline of the crustal dust input. A weakening of the westerlies has been invoked by other authors to explain the decrease of the dust concentration in TP ice cores during the 20th century. For instance, the Ca concentrations (Ca is a proxy of TP dust) of the Geladaindong core declined gradually since the early 1900s and more abruptly after 1950 (Grigholm et al., 2015) coinciding with a reduction of the dust storm activity across the TP (Qian et al., 2002; Shao and Dong, 2006; Li et al., 2012). Several authors (Fu et al. (2008), Goudie (2009), Wu et al., 2013 and Zhang et al. (2015)) related the post-1950 dust storm frequency decrease to the weakening of the westerly winds over the TP due to a change in the winter NAO phase. A weak Siberian High due to warmer climate conditions in the 20th century precluded cyclogenesis in the arid regions of north China which also decreased the frequency of dust storms (Yang et al., 2007). This decreasing lithogenic input to the Puruogangri surface and its association with large-scale modes of climate variability likely lead to greater visibility of the 20th century anthropogenic signal in the core. Thus, the EF trends over the last century can be discussed in terms of the strength of anthropogenic emissions, possible sources and geographical origin.

In order to seasonally constrain the geographical atmospheric influence specifically for the Puruogangri ice cap, a 7-day NOAA HYSPLIT back-trajectory frequency analysis was performed over the 1948–1992 period for every day of January (middle of the dry season) and July (middle of the wet season). As expected, the highest density of trajectories follows an eastward direction in winter (Fig. 6a), pointing to the Thar Desert (Rajasthan, India), central Asia (e.g., Pakistan, Afghanistan), Former Soviet Union (FSU) (e.g., Kyrgyzstan, Tajikistan, Uzbekistan, and Turkmenistan) and Middle East countries (e.g., Iran, Iraq) and their extensive networks of metallurgical facilities (Fig. 6) as possible additional sources of contaminants to Puruogangri. Notably, Kyrgyzstan contains the largest number of Sb mining and smelting facilities in central Asia (Baker et al., 2010). In summer, the monsoonal influence dominates the less prominent zonal circulation, leading multiple trajectories around the ice cap (Fig. 6b). Pollutants from South and East Asia (e.g., India and China) can then, although not consistently, be transported further inland into Tibet and scavenged by snow precipitation (Cong et al., 2010a, 2010b; Lüthi et al., 2015).

Between 1900 and 1992, Cd, Sb, Ag, Pb and Zn present a significant enrichment increase of respectively 40%, 40%, 30%, 30% and 20% relative to the pre-1900 median (Table 1, Fig. 5a) suggesting an anthropogenic contribution. However, the rate of increase is not consistent throughout the 20th century, and each TE shows different trends at the sub-decadal scale. For the five TEs, Figs. 7, 8 and 9 display the 5-year average of annual median EFs above their respective pre-1900 median over the 1850–1992 period. Tl EF also increases significantly during the 20th century (Fig. C). However, its increase only reaches 10% and is therefore not discussed in detail.

Three periods can be distinguished within the 20th century contamination time series: (1) the pre-1935 period when the enrichment is most noticeable for Sb and Cd but within the 1497–1900 range of variability; (2) the 1935–1980 period during which the enrichment of all five TEs (Ag, Zn, Pb, Cd and Sb) increases strongly and then declines rapidly after 1965; and (3) the most recent part of the record (1980–1992) when EFs are rising again. In order to identify the geographical sources and the processes responsible for the contamination, EF trends are examined in the light of metallurgy and fossil fuel production rates and compared with available anthropogenic emissions data in Figs. 7, 8, 9.

3.3.1. The 1900–1935 period: minimal but sustained Sb and Cd enrichment

In the early 1900s, Sb remains enriched above the pre-1900 median with EF values resembling those of the 1497–1900 period (EF = 3.4 in 1905) (Fig. 7). Cd exhibits a similar trend to that of Sb with an EF above the pre-1900 median (Fig. 8) but neither of them exceed the range of the 1497–1900 values (Fig. 5). During this period (especially between 1925 and 1935) the high dust concentration is not reflected in the crustal (EOF 1) or evaporitic (EOF 2) components of the TEs budget (Fig. B). This means that the Sb and Cd enrichment could either reflect a change in the nature of the crustal dust or truly point to an, although weak, anthropogenic contamination of the ice. The volatility of Sb makes it one of the primary vapor phase products of high-temperature industrial and/or metallurgic processes (Yan et al., 2001; Wang and Tomita, 2003; Merian et al., 2004; Reddy et al., 2005, Vejahati et al., 2010) such as: coal combustion in electric power plants, gasoline combustion, refuse incineration, lead smelting, and steel-iron production (Austin and Millward, 1988; Nriagu and Pacyna, 1988; Swaine, 2000; Pacyna and Pacyna, 2001; Krachler et al., 2005; Tian et al., 2011). Cd is also a volatile component of coal burning products (fly ash) although it is emitted to the atmosphere in lower concentrations than Sb (Querol et al., 1995; Yan et al., 2001; Xu et al., 2004). Thus, Sb and Cd as coal-burning products are good candidates for long-range atmospheric transport and deposition on remote TP glaciers. To date, very few Third Pole ice core archives have reported a Sb atmospheric contamination prior to 1935. Hong et al. (2009) extracted an 800-year long Sb record from a Mt. Everest ice core (Himalaya) and proposed the relationship between the substantial increase in Indian coal production and a slight Sb enrichment in the ice in the early 1900s. On the northern side of the TP, for the Belukha ice core (Altai), Eichler et al. (2014) related the 19th and early 20th century Sb enrichment to regional (Russian Altai) smelting activities. At the turn of the 20th century, the first producers and consumers of coal were the western European countries and members of the Organization for Economic Co-operation and Development (OECD). Coal production data (HYDE, PBL Netherlands Environmental Assessment Agency, 2015), also shown in Fig. 7, clearly indicate that OECD countries (western Europe) were dominating worldwide production and were then a likely source of the early Sb contamination of the Puruogangri ice cap. In the Chinese historical context, coal combustion has supported the "Westernization" of China's economy (since the 1860s) (Wang et al., 2010) and the acceleration of warfare production following the first Sino-Japanese war (1894–95). Consequently, the domestic coal burning emission could be partly responsible for the enrichment of Sb and Cd at the turn of the 20th century.

3.3.2. The 1935–1980 period: fossil fuel contributions and metallurgy

3.3.2.1. Antimony. The most significant enrichments in Sb occur in 1935–1950 (EF_{max} 1940 = 4) and 1960–1980 (EF_{max} 1965 = 4.7) which respectively equate to a 100% and a 135% increase of the pre-1900 enrichment (Fig. 7). The post-1935 Sb EF trend in the Puruogangri record is consistent with what was observed in other cores from the regions surrounding the TP (Altai (Eichler et al., 2014), Pamir (Li et al., 2006) and Tien Shan (Liu et al., 2011)). The Puruogangri record most strongly

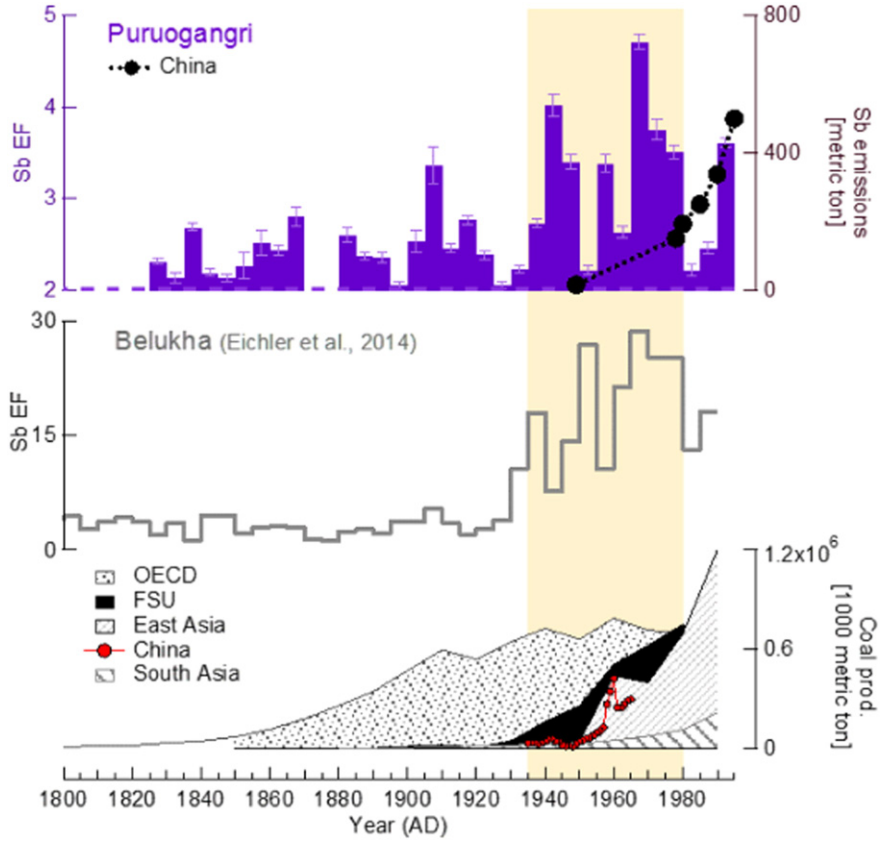

Fig. 7. Comparison between the Puruogangri 5-year average EF of Sb above the pre-1900 median (purple dotted line) with the Belukha ice core record (Russia, Eichler et al., 2014) and with China Sb emission (Tian et al., 2012) and coal production data (HYDE database, 2015; Chang (1970) for China coal production).

resembles atmospheric Sb derived from the Belukha glacier (Fig. 7) on the northern border of the Third Pole region, in the Altai Mountains (Eichler et al., 2014). In the Belukha core, coal burning, and especially regional metallurgic activities (Cu-Ni and steel-iron production) of the FSU, accounted for the steep increase of Sb concentration from 1935 to a maximum in 1970. In the Tien Shan region (Northern China), Sb atmospheric input increased in the 1950s and reached a maximum in the 1980s as observed in the Miaoergou ice core (Liu et al., 2011). The Miaoergou post-1953 enrichment in Sb is associated with anthropogenic emissions from Eurasia transported by westerly atmospheric circulation. On Puruogangri, the post-1935 Sb enrichment also coincides with the trend of Soviet coal production which increased rapidly after 1930. Moreover, the absolute maximum around the mid-1960s followed by the decline towards the 1980s reflects the industrial emission trends of the FSU reconstructed by Eichler et al. (2014). This makes FSU coal burning and metallurgy a plausible combination of sources of atmospheric Sb for the central TP during the second part of the 20th century. Notably, a secondary maximum in Sb EF observed in 1955–1960, coincides with an acceleration of Chinese coal production during the years of the Great Leap Forward (1958–1961) (Chang, 1970). Thus, a contribution of industrial emissions from China since the 1950s to the Sb measured in Puruogangri cannot be ruled out. However, more information is needed to confidently assess the geographical provenance of the Sb pollution. South Asia emissions (Fig. 7) could also have contaminated Puruogangri but to a lesser extent than the Everest core where the pronounced increase of Sb contamination in the 1970s was attributed to fossil fuel combustion and to nonferrous metal production in India (Hong et al., 2009). Atmospheric pollutants reaching Everest are mainly transported by monsoonal incursions that do not consistently (low frequency back-trajectories, Fig. 6b) penetrate inland as far as central Tibet (Ramanathan et al., 2007; Kaspari et al., 2009a, 2009b).

3.3.2.2. Cadmium, thallium and zinc. For Cd, the second highest peak in enrichment occurs between 1935 and 1945 ($EF_{max}1940 = 4.7$) in the Puruogangri core (Fig. 8) when coal production was accelerating in the FSU (Fig. 7). In an ice core from Greenland (McConnell and Edwards, 2008), a maximum in Cd concentration was detected around 1946 and linked to the higher rate of fossil fuel combustion at a hemispheric scale (McConnell and Edwards, 2008; Olendrzyński et al., 1996). Products from this intense global fossil fuel combustion, including gasoline combustion from distant sources, could also have been deposited on the Puruogangri surface between 1935 and 1950 and led to part of the Cd contamination. The argument that the ice cap also received coal emission products during the 1935–1950 period is supported by the high enrichment in Tl (Fig. C) which is also a volatile element emitted during coal combustion (Antón et al., 2013).The highest Tl EF peak occurs in 1940 (Tl $EF_{max} = 2.4$) while the 1965 peak ($EF = 2.1$) is only the second highest (Fig. C).

Cd is also an atmospheric product of metallurgical processes. Nonferrous metal production, and especially Zn smelting, is the main anthropogenic source of Cd and Zn in the environment (Pacyna and Pacyna, 2001; Bi et al., 2006), and primary Zn smelting accounts for the largest proportion of Zn emissions in the non-ferrous metal smelting category. Zn enrichment is only visible after 1940 and peaked around the same time as Cd in 1965 (Zn $EF_{max} = 2.8$; Cd $EF_{max} = 5.2$). The FSU Zn primary production data illustrated in Fig. 8 show a strong Spearman correlation with Cd EF ($r = 0.59$ ($p = 0.1$)) and with Zn EF trends ($r = 0.57$ ($p = 0.1$)). These correlations support the hypothesis that the post-1950 Cd and Zn contamination on Puruogangri could have partly originated from the FSU metallurgical industries. Eichler et al. (2014) also identified the extensive Soviet metallurgical industrial complex as the main source of Cd and Zn in the Belukha core after 1935 and could reconstruct the trend of Cd FSU emissions from the ice

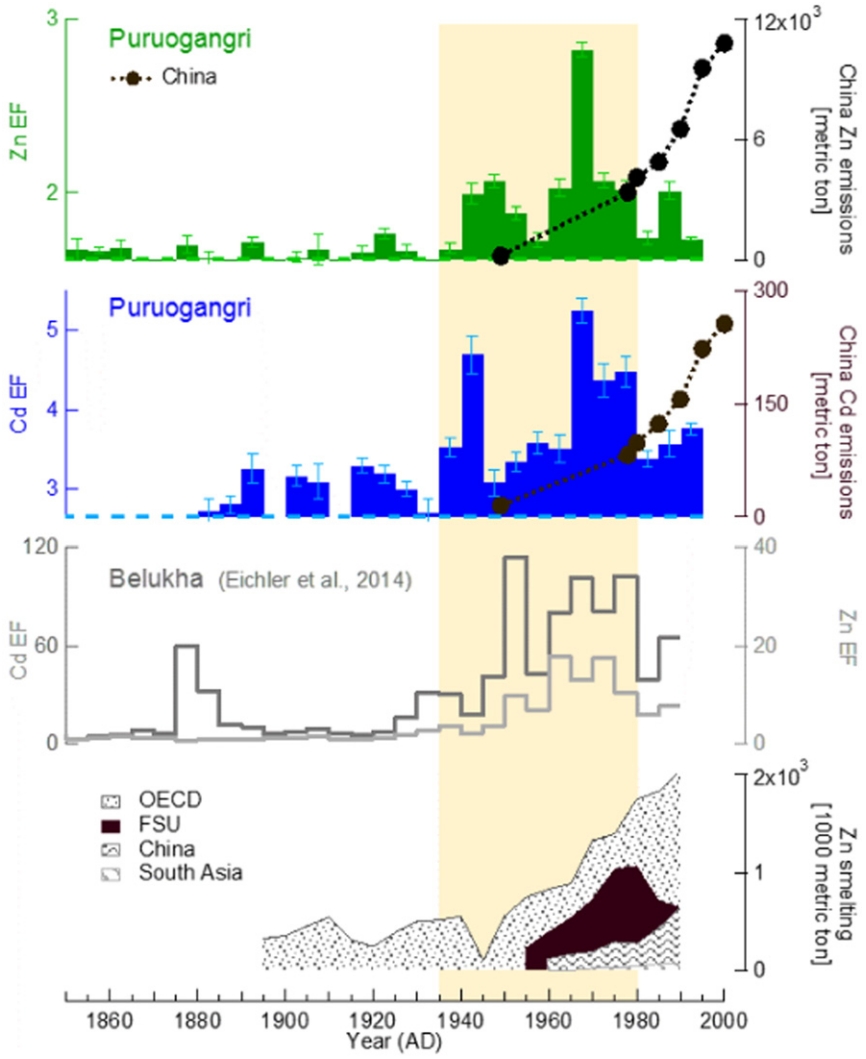

Fig. 8. Comparison between the Puruogangri 5-year average EF Zn and Cd above the pre-1900 median (green and blue dotted lines) with the Belukha ice core record (Russia, Eichler et al., 2014) and with China emission (Tian et al., 2012) and Zn-smelting production data (HYDE database, 2015).

core record (Fig. 8). Kazakhstan, along with Russia, were the major Zn-producing republics of the FSU, mining 50% and smelting 50% of the Zn in the FSU (Farmer and Farmer, 2000; USGS, 1995). Many of the production plants are located in southeastern Kazakhstan (Fig. 6) which places the very volatile Zn and Cd particles in the pathway of westerly winds affecting the central TP. The Cd and Zn FSU emissions data by Eichler et al. (2014) indicate that the FSU was a stronger emitter than China in the 1960s–70s, which coincides with the FSU's most prolific Zn smelting period (Fig. 8).

3.3.2.3. Lead and silver. Through the 20th century, the Pb EF has a more unusual variability than other enriched TEs (Fig. 9). For instance, the 1935–1950 enrichment above the pre-1900 median is not seen in the Pb record despite FSU coal production which doubled during that period (Fig. 7). This suggests that the anthropogenic contribution is masked by the crustal Pb prior to 1950. Furthermore, Ag is a reported by-product of Pb extraction (Merian et al., 2004). Ag enrichment on Puruogangri, being similar to that of Pb, suggests that the FSU metallurgical trends could have triggered the 1950 onset of a significant Pb and Ag atmospheric contamination of the central TP (Fig. 9). Another possible contributor to the Pb and Ag contamination of the Puruogangri ice could have been the Chinese provincial iron and steel smelting activities which tripled the national production between 1957 and 1960 (Li and Yang, 2005; Tian et al., 2015). This surge in Chinese steel output accompanied the Great Leap Forward when agricultural workers of all provinces were assigned to backyard steel smelters (Chang, 1970). The provincial steel production collapsed in 1962 but regenerated around 1966 at the beginning of the Chinese Cultural Revolution (1966–1976). Although the Chinese steel production was three orders of magnitude smaller than that of the FSU, its relative proximity to the Puruogangri ice cap could make it a relevant source of atmospheric Pb and Ag particles.

The Pb EF reaches a maximum in the 1970s (Pb $EF_{max} = 3.6$) then declines in the 1980s, possibly reflecting the FSU industrial slowdown while South and East Asian industrial activities were on the rise. Yet, the worldwide Pb emissions from fossil fuel combustion far outweighed those from all other sources combined during the 1960s and 1970s (Swaine, 2000; Gustafsson et al., 2009) and are recorded in central Greenland ice (Barbante et al., 2003; Reddy et al., 2005) but also in Qinghai Lake sediments (Jin et al., 2010). Therefore, the worldwide combustion of leaded gasoline could be considered as an additional source of Pb for the central TP from 1950 to 1980. This hypothesis is consistent with the Pb trend reported for Everest being associated with South Asian leaded gasoline combustion (Lee et al., 2011).

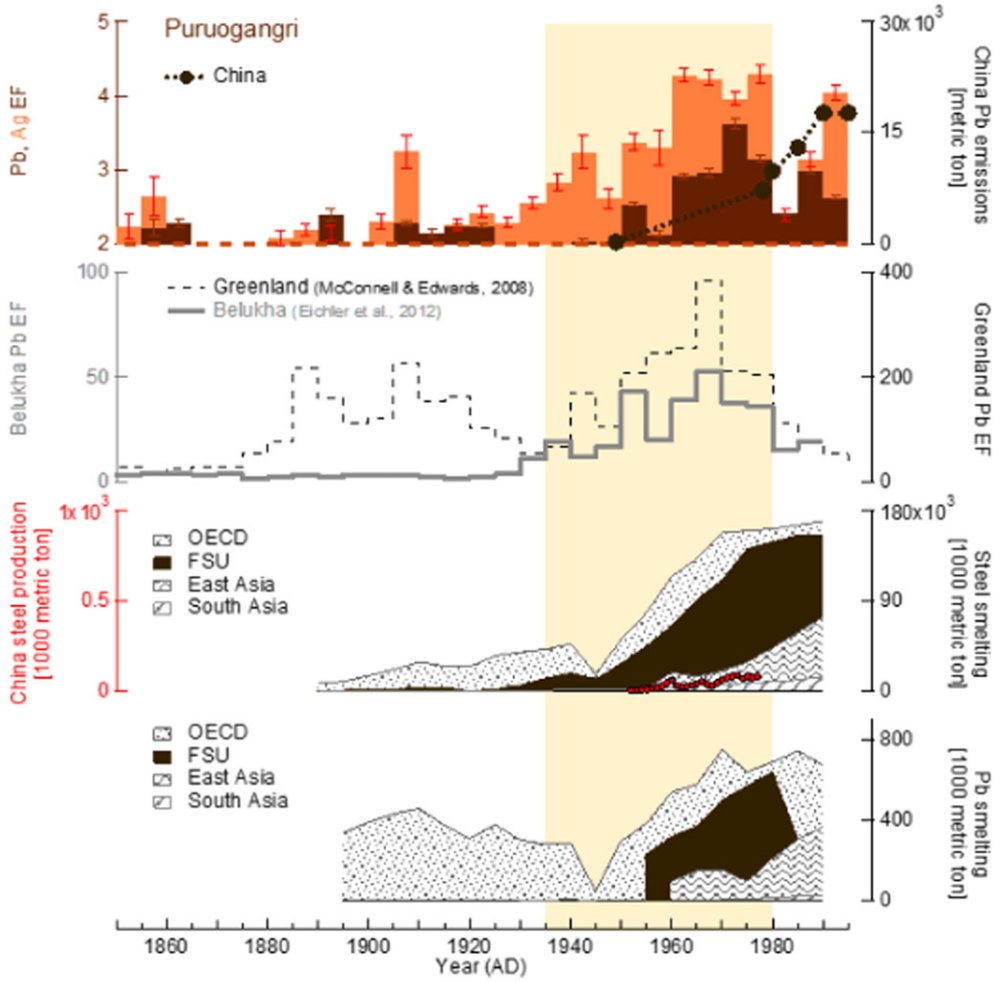

Fig. 9. Comparison between the Puruogangri 5-year average EF Pb and Ag above the Pb pre-1900 median (brown dotted lines) with ACT2 (Greenland, McConnell and Edwards, 2008)), Everest (Himalaya, Lee et al., 2011) and with Pb emission (Tian et al., 2012) and Pb and steel production data (HYDE database, 2015; Li and Yang (2005) for the Chinese steel production data).)

3.3.3. The 1980–1992 period: a possible new Asian input

In the 1980s, the contamination content falls back to its 1950 level for Sb EF, Cd EF, Zn EF and Pb EF and even below the pre-1900 median value for Ag EF. A subsequent increase in EFs is observed for the most recent decade of the Puruogangri record. This pattern coincides with the beginning of the rise in Chinese emissions (Tian et al., 2012) especially those of Sb, Cd and Pb. However, the FSU emissions of Zn (Eichler et al., 2014) could still explain the secondary Zn EF peak of 1985 followed by the drop in Zn contamination at the top of the ice core record. Among the anthropogenic processes previously implicated in the atmospheric pollutant deposition to Puruogangri, coal productions of South and especially East Asia stand out as the fastest growing contributors (Fig. 7) (Flegal et al., 2013). Compared to the other regions, Chinese Zn, steel and Pb smelting production increase exponentially in the 1990s, which makes them a more likely source of Zn, Cd, Pb and Ag to the central TP. Although their production volumes were not as large as those of the western and FSU metallurgical industries, East Asian industrial and mining production was already substantial in the 1960s. The hypothesis that Puruogangri ice captures pollution from the west until 1980 and records the first indications of the South and East Asian contribution afterwards is consistent with the fact that, despite its remoteness, the Puruogangri ice cap is located at the crossroads of atmospheric contaminant trajectories and this glacier is thus under both westerly and south-easterly atmospheric influences.

4. Conclusion

The extraction of a 500-year TE record from the Puruogangri ice core provides a highly resolved account of the impact of past atmospheric influences, environmental processes and human activities on the central TP. The terrestrial aerosols (including a substantial proportion of evaporitic salts) overwhelm the elemental budget; only 3% of the variability is controlled by non-crustal sources. The anthropogenic input becomes relevant only during the 20th century and particularly after 1935 when Sb, Cd, Zn, Pb and Ag are significantly enriched in the ice relative to the pre-industrial background. Anthropogenic Sb is found to be the marker of the northern hemisphere coal combustion since 1935, including the Chinese coal combustion during the Great Leap Forward. Cd and Zn emissions from the FSU Zn smelting possibly added to their emission from FSU coal burning after 1935 while Pb and Ag contaminate the central TP since 1950 as products of increase in steel and Pb smelting activities in China and in central and South Asia. The maximum anthropogenic Sb, Cd, Zn and Pb deposition found in the Puruogangri ice core occurs in 1965. The beginning of a new increase at the top of the record (after 1985), synchronous with the East and South Asia emission trends, is the likely indication that Puruogangri records the new era of atmospheric heavy metals pollution linked to the economic emergence of China and India as well as other regions bordering the TP on the east and south. In this latter case, the summer monsoon circulation would then be expected to have marginalized the winter westerlies and

become the main conveyor of atmospheric Sb, Cd, Zn, Pb and Ag to the TP. In light of the 500-year record presented in this study, examination of ice core archives covering the last two decades (i.e., the post-1992 period) would allow corroboration of the prominent role of the meridional (or monsoonal) circulation in transporting pollution and bring new data to the ongoing debate on the role of anthropogenic aerosols in the shift of the summer monsoon rain belt in China. We estimate that Pb isotopes as well as black carbon measurements of the Puruogangri ice core would make valuable complements to this study in terms of geographical source apportionment and the impact on the glacial energy balance and atmospheric radiative forcing.

Acknowledgements

We thank all the participants in the Puruogangri 2000 field program from the Byrd Polar and Climate Research Center (BPCRC, USA) and from the Laboratory of Ice Core and Cold Regions Environment (LICCRE, China). We thank Anja Eichler and Joseph McConnell who provided the trace elements data for the Belukha and the ACT2 ice cores. The input of Julien Nicolas for the calculation of the backtrajectory frequencies, Stacy Porter and Henry Brecher for editing is gratefully acknowledged. We appreciate the comments of three anonymous reviewers and our editor, Filip Tack. Financial support to the "Third Pole Project" was provided by the NSF Atmospheric Chemistry and Physics program (award #1149239) and by The Ohio State University (Byrd Polar Fellowship). This is Byrd Polar and Climate Research Center contribution #1568. The published data are now available on the NOAA paleoclimatology database at https://www.ncdc.noaa.gov/paleo/study/22214.

Appendix A. Supplementary data

Supplementary data to this article can be found online at http://dx.doi.org/10.1016/j.scitotenv.2017.05.195.

References

Aizen, V., Mayewski, P., Aizen, E., Joswiak, D., Surazakov, A., Kaspari, S., Grigholm, B., Krachler, M., Handley, M., Finaev, A., 2009. Stable-isotope and trace element time series from Fedchenko glacier (Pamirs) snow/firn cores. J. Glaciol. 55, 275291.

An, W., Hou, S., Zhang, W., Wang, Y., Liu, Y., Wu, S., Pang, H., 2016. Significant recent warming over the northern Tibetan Plateau from ice core $\delta^{18}O$ records. Clim. Past 12, 201–211.

Antón, M., Spears, D., Somoano, M., Tarazona, M., 2013. Thallium in coal: analysis and environmental implications. Fuel 105, 13–18.

Austin, L.S., Millward, G.E., 1988. Simulated effects of tropospheric emissions on the global antimony cycle. Atmos. Environ. 22, 1395–1403 1967.

Baker, M.S., Elias, N., Guzmán, E., Soto-Viruet, Y., 2010. Mineral facilities of Northern and Central Eurasia: U.S. Geological Survey Open-File Report 1255.

Barbante, C., Boutron, C.F., Morel, C., Ferrari, C., Jaffrezo, J.L., Cozzi, G., Gaspari, V., Cescon, P., 2003. Seasonal variations of heavy metals in central Greenland snow deposited from 1991 to 1995. J. Environ. Monit. 5, 328–335.

Bauer, K., 2006. Common property and power: insights from a spatial analysis of historical and contemporary pasture boundaries among pastoralists in Central Tibet. J. Polit. Ecol.

Bi, X., Feng, X., Yang, Y., Qiu, G., Li, G., 2006. Quantitative assessment of cadmium emission from zinc smelting and its influences on the surface soils and mosses in Hezhang County, Southwestern China. Atmos. Environ. 40, 4228–4233.

Bollasina, M., Ming, Y., Ramaswamy, V., Schwarzkopf, M., Naik, V., 2014. Contribution of local and remote anthropogenic aerosols to the twentieth century weakening of the South Asian Monsoon. Geophys. Res. Lett. 41, 680–687.

Bonasoni, P., Laj, P., Marinoni, A., Sprenger, M., Angelini, F., Arduini, J., et al., 2010. Atmospheric Brown Clouds in the Himalayas: first two years of continuous observations at the Nepal Climate Observatory-Pyramid (5079 m). Atmos. Chem. Phys. 10, 7515–7531.

Chang, K.-S., 1970. Nuclei-formation of communist China's iron and steel industry. Ann. Assoc. Am. Geogr. 60, 257–283.

Chen, P., Kang, S., Bai, J., Sillanpää, M., Li, C., 2015. Yak dung combustion aerosols in the Tibetan Plateau: chemical characteristics and influence on the local atmospheric environment. Atmos. Res. 156, 5866.

Chu, G., Sun, Q., Wang, X., Sun, J., 2008. Snow anomaly events from historical documents in eastern China during the past two millennia and implication for low-frequency variability of AO/NAO and PDO. Geophys. Res. Lett. 35.

Cong, Z., Kang, S., Liu, X., Wang, G., 2007. Elemental composition of aerosol in the Nam Co region, Tibetan Plateau, during summer monsoon season. Atmos. Environ. 41, 1180–1187.

Cong, Z., Kang, S., Dong, S., Liu, X., Qin, D., 2010a. Elemental and individual particle analysis of atmospheric aerosols from high Himalayas. Environ. Monit. Assess. 160, 323–335.

Cong, Z., Kang, S., Zhang, Y., Li, X., 2010b. Atmospheric wet deposition of trace elements to central Tibetan Plateau. Appl. Geochem. 25, 1415–1421.

Cong, Z., Kang, S., Zhang, Y., Gao, S., Wang, Z., Liu, B., Wan, X., 2015. New insights into trace element wet deposition in the Himalayas: amounts, seasonal patterns, and implications. Environ. Sci. Pollut. Res. 22, 2735–2744.

Craddock, P., Gurjar, L., Hegde, K., 2010. Zinc production in medieval India. World Archaeol. 15, 211–217.

Currell, M., Cartwright, I., Raveggi, M., Han, D., 2011. Controls on elevated fluoride and arsenic concentrations in groundwater from the Yuncheng Basin, China. Appl. Geochem. 26, 540–552.

Davis, M., Thompson, L., Yao, T., Wang, N., 2005. Forcing of the Asian monsoon on the Tibetan Plateau: evidence from high-resolution ice core and tropical coral records. J. Geophys. Res. 110.

Dean, W., 1987. Trace and Minor Elements in Evaporites. SC4. The Society of Economic Paleontologists and Mineralogists (SEPM) Marine Evaporites.

Dean, W., 2013. Encyclopedia of Marine Geosciences.

Duce, R.A., Hoffman, G.L., Zoller, W.H., 1975. Atmospheric trace metals at remote northern and southern hemisphere sites: pollution or natural? Science 187, 59–61.

Eichler, A., Olivier, S., Henderson, K., Laube, A., Beer, J., Papina, T., Gäggeler, H., Schwikowski, M., 2009. Temperature response in the Altai region lags solar forcing. Geophys. Res. Lett. 36.

Eichler, A., Tobler, L., Eyrikh, S., Gramlich, G., Malygina, N., Papina, T., Schwikowski, M., 2012. Three centuries of Eastern European and Altai lead emissions recorded in a Belukha ice core. Environ. Sci. Technol. 46, 4323–4330.

Eichler, A., Tobler, L., Eyrikh, S., Malygina, N., Papina, T., Schwikowski, M., 2014. Ice-core based assessment of historical anthropogenic heavy metal (Cd, Cu, Sb, Zn) emissions in the Soviet Union. Environ. Sci. Technol. 48, 2635–2642.

Erel, Y., Dayan, U., Rabi, R., Rudich, Y., Stein, M., 2006. Trans boundary transport of pollutants by atmospheric mineral dust. Environ. Sci. Technol. 40, 2996–3005.

Fan, Q., Lai, Z., Long, H., Sun, Y., Liu, X., 2010. OSL chronology for lacustrine sediments recording high stands of Gahai Lake in Qaidam Basin, northeastern Qinghai–Tibetan Plateau. Quat. Geochronol. 5, 223–227.

Farmer, A.A., Farmer, A.M., 2000. Concentrations of cadmium, lead and zinc in livestock feed and organs around a metal production centre in eastern Kazakhstan. Sci. Total Environ. 257, 53–60.

Ferrari, C., Clotteau, T., Thompson, L., Barbante, C., Cozzi, G., Cescon, P., Hong, S., Maurice-Bourgoin, L., Francou, B., Boutron, C., 2001. Heavy metals in ancient tropical ice: initial results. Atmos. Environ. 35, 58095815.

Flegal, R., Gallon, C., Ganguli, P., Conaway, C., 2013. All the lead in China. Crit. Rev. Environ. Sci. Technol. 43, 1869–1944.

Fu, P., Huang, J., Li, C., Zhong, S., 2008. The properties of dust aerosol and reducing tendency of the dust storms in northwest China. Atmos. Environ. 42, 5896–5904.

Gabrielli, P., Barbante, C., Boutron, C., Cozzi, G., Gaspari, V., Planchon, F., Ferrari, C., Turetta, C., Hong, S., Cescon, P., 2005. Variations in atmospheric trace elements in Dome C (East Antarctica) ice over the last two climatic cycles. Atmos. Environ. 39, 6420–6429.

Gabrielli, P., Cozzi, G., Torcini, S., Cescon, P., Barbante, C., 2008. Trace elements in winter snow of the Dolomites (Italy): a statistical study of natural and anthropogenic contributions. Chemosphere 72, 1504–1509.

Gabrielli, P., Hardy, D., Kehrwald, N., Davis, M., Cozzi, G., Turetta, C., Barbante, C., Thompson, L., 2014. Deglaciated areas of Kilimanjaro as a source of volcanic trace elements deposited on the ice cap during the late Holocene. Quat. Sci. Rev. 93, 110.

Gao, J., Risi, C., Masson-Delmotte, V., He, Y., Xu, B., 2016. Southern Tibetan Plateau ice core $\delta^{18}O$ reflects abrupt shifts in atmospheric circulation in the late 1970s. Clim. Dyn. 46, 291–302.

Goudie, A., 2009. Dust storms: recent developments. J. Environ. Manag. 90, 89–94.

Grigholm, B., Mayewski, P., Kang, S., Zhang, Y., Morgenstern, U., Schwikowski, M., et al., 2015. Twentieth century dust lows and the weakening of the westerly winds over the Tibetan Plateau. Geophys. Res. Lett. 42, 2434–2441.

Grigholm, B., Mayewski, P.A., Aizen, V., Kreutz, K., Wake, C.P., Aizen, E., Kang, S., Maasch, K.A., Handley, M.J., Sneed, S.B., 2016. Mid-twentieth century increases in anthropogenic Pb, Cd and Cu in central Asia set in hemispheric perspective using Tien Shan ice core. Atmos. Environ. 131, 17–28.

Guo, Q., 2012. Hydrogeochemistry of high-temperature geothermal systems in China: a review. Appl. Geochem. 27, 1887–1898.

Guo, Q., Wang, Y., 2009. Trace element hydrochemistry indicating water contamination in and around the Yangbajing geothermal field, Tibet, China. B Environ. Contam. Tox 83, 608–613.

Guo, Q., Wang, Y., Liu, W., 2009. Hydrogeochemistry and environmental impact of geothermal waters from Yangyi of Tibet, China. J. Volcanol. Geotherm. Res. 180, 9–20.

Gustafsson, O., Kruså, M., Zencak, Z., Sheesley, R.J., Granat, L., Engström, E., Praveen, P.S., Rao, P.S., Leck, C., Rodhe, H., 2009. Brown clouds over South Asia: biomass or fossil fuel combustion? Science 323, 495–498.

Han, Y., Fang, X., Zhao, T., Bai, H., Kang, S., Song, L., 2009. Suppression of precipitation by dust particles originated in the Tibetan Plateau. Atmos. Environ. 43, 568–574.

Hegde, K., 1989. Zinc and brass production in ancient India. Interdiscip. Sci. Rev. 14, 86–96.

Hillman, A., Yu, J., Abbott, M., Cooke, C., Bain, D., Steinman, B., 2014. Rapid environmental change during dynastic transitions in Yunnan Province, China. Quat. Sci. Rev. 98, 24–32.

Hillman, A., Abbott, M., Yu, J., Bain, D., Chiou-Peng, T., 2015. Environmental legacy of copper metallurgy and Mongol silver smelting recorded in Yunnan Lake sediments. Environ. Sci. Technol. 49, 3349–3357.

Hinkley, T., Lamothe, P., Wilson, S., Finnegan, D., Gerlach, T., 1999. Metal emissions from Kilauea, and a suggested revision of the estimated worldwide metal output by quiescent degassing of volcanoes. Earth Planet Sci. Lett. 170, 315–325.
Hong, S., Lee, K., Hou, S., Hur, S., Ren, J., Burn, L., Rosman, K., Barbante, C., Boutron, C., 2009. An 800-year record of atmospheric As, Mo, Sn, and Sb in central Asia in high-altitude ice cores from Mt. Qomolangma (Everest), Himalayas. Environ. Sci. Technol. 43, 8060–8065.
Hou, Z., Cook, N.J., 2009. Metallogenesis of the Tibetan collisional orogen: a review and introduction to the special issue. Ore Geol. Rev.
Huang, X., Sillanpää, M., Duo, B., Gjessing, E., 2008. Water quality in the Tibetan Plateau: metal contents of four selected rivers. Environ. Pollut. Barking Essex 156.
Hudson, A., Quade, J., 2013. Long-term east-west asymmetry in monsoon rainfall on the Tibetan Plateau. Geology 41, 351–354.
Huss, M., Farinotti, D., 2012. Distributed ice thickness and volume of all glaciers around the globe. J. Geophys. Res. Earth Surf. 117 2003. (2012 n/a–n/a).
HYDE database, 2015. History Database of the Global Environment. http://themasites.pbl.nl/tridion/en/themasites/hyde/productiondata/index-2.html.
Indoitu, R., Orlovsky, L., Orlovsky, N., 2012. Dust storms in Central Asia: spatial and temporal variations. J. Arid Environ. 85, 62–70.
Jin, Z., Han, Y., Chen, L., 2010. Past atmospheric Pb deposition in Lake Qinghai, northeastern Tibetan Plateau. J. Paleolimnol. 43, 551–563.
Joswiak, D., Yao, T., Wu, G., Tian, L., Xu, B., 2013. Ice-core evidence of westerly and monsoon moisture contributions in the central Tibetan Plateau. J. Glaciol. 59, 56–66 (11).
Kang, S., Mayewski, P., Qin, D., Yan, Y., Hou, S., Zhang, D., Ren, J., Kruetz, K., 2002. Glaciochemical records from a Mt. Everest ice core: relationship to atmospheric circulation over Asia. Atmos. Environ. 36, 33513361.
Kang, S., Zhang, Q., Kaspari, S., Qin, D., Cong, Z., Ren, J., Mayewski, P., 2007. Spatial and seasonal variations of elemental composition in Mt. Everest (Qomolangma) snow/firn. Atmos. Environ. 41, 72087218.
Kang, S., Zhang, Y., Zhang, Y., Grigholm, B., Kaspari, S., Qin, D., Ren, J., Mayewski, P., 2010. Variability of atmospheric dust loading over the central Tibetan Plateau based on ice core glaciochemistry. Atmos. Environ. 44, 2980–2989.
Kang, S., Huang, J., Wang, F., Zhang, Q., Zhang, Y., Li, C., et al., 2016. Atmospheric mercury depositional chronology reconstructed from Lake sediments and ice core in the Himalayas and Tibetan Plateau. Environ. Sci. Technol. 50, 2859–2869.
Kaspari, S., Mayewski, P., Handley, M., Kang, S., Hou, S., Sneed, S., Maasch, K., Qin, D., 2009a. A high-resolution record of atmospheric dust composition and variability since A.D. 1650 from a Mount Everest ice core. J. Clim. 22, 3910–3925.
Kaspari, S., Mayewski, P., Handley, M., Osterberg, E., Kang, S., Sneed, S., Hou, S., Qin, D., 2009b. Recent increases in atmospheric concentrations of Bi, U, Cs, S and Ca from a 350-year Mount Everest ice core record. J. Geophys. Res. 114.
Krachler, M., Zheng, J., Koerner, R., Zdanowicz, C., Fisher, D., Shotyk, W., 2005. Increasing atmospheric antimony contamination in the northern hemisphere: snow and ice evidence from Devon Island, Arctic Canada. J. Environ. Monit. 7, 1169–1176.
Krachler, M., Zheng, J., Fisher, D., Shotyk, W., 2009. Global atmospheric As and Bi contamination preserved in 3000 year old Arctic ice. Glob. Biogeochem. Cy 23 (n/a–n/a).
Kreutz, K., Sholkovitz, E., 2000. Major element, rare earth element, and sulfur isotopic composition of a high-elevation firn core: sources and transport of mineral dust in central Asia. Geochem. Geophys. Geosyst. 1 (n/a–n/a).
Lafitte, G., 2013. Spoiling Tibet: China and Resource Nationalism on the Roof of the World. Zed Books, London.
Lambert, G., Cloarec, M.-F., Pennisi, M., 1988. Volcanic output of SO_2 and trace metals: a new approach. Geochim. Cosmochim. Ac 52, 39–42.
Le Cloarec, M.F., Allard, P., Ardouin, B., 1992. Radioactive isotopes and trace elements in gaseous emissions from White Island, New Zealand. Earth Planet. Sci. Lett. 108, 19–28.
Lee, K., Hur, S., Hou, S., Hong, S., Qin, X., Ren, J., Liu, Y., Rosman, K., Barbante, C., Boutron, C., 2008a. Atmospheric pollution from trace elements in the remote high-altitude atmosphere in central Asia as recorded in snow from Mt. Qomolangma (Everest) of the Himalayas. Sci. Total Environ. 404, 171–181.
Lee, C., Qi, S., Zhang, G., Luo, C., Zhao, L., Li, X., 2008b. Seven thousand years of records on the mining and utilization of metals from lake sediments in Central China. Environ. Sci. Technol. 42, 4732–4738.
Lee, K., Hur, S., Hou, S., Burn-Nunes, L., Hong, S., Barbante, C., Boutron, C., Rosman, K., 2011. Isotopic signatures for natural versus anthropogenic Pb in high-altitude Mt. Everest ice cores during the past 800 years. Sci. Total Environ. 412–413, 194–202.
Li, W., Yang, D.T., 2005. The great leap forward: anatomy of a central planning disaster. J. Polit. Econ.
Li, Z., Yao, T., Tian, L., Xu, B., Li, Y., 2006. Atmospheric Pb variations in Central Asia since 1955 from Muztagata ice core record, eastern Pamirs. Chin. Sci. Bull. 51, 1996–2000.
Li, C., Kang, S., Zhang, Q., 2009. Elemental composition of Tibetan Plateau top soils and its effect on evaluating atmospheric pollution transport. Environ. Pollut. 157, 2261–2265.
Li, C., Kang, S., Zhang, Q., Gao, S., 2012. Geochemical evidence on the source regions of Tibetan Plateau dusts during non-monsoon period in 2008/09. Atmos. Environ. 59, 382–388.
Liu, Y., Hou, S., Hong, S., Hur, S., Lee, K., Wang, Y., 2011. High-resolution trace element records of an ice core from the eastern Tien Shan, central Asia, since 1953 AD. J. Geophys. Res. Atmos. 116 (1984–2012).
Lüthi, Z., Škerlak, B., Kim, S.-W., Lauer, A., Mues, A., Rupakheti, M., Kang, S., 2015. Atmospheric brown clouds reach the Tibetan Plateau by crossing the Himalayas. Atmos. Chem. Phys. 15, 6007–6021.
Marx, S.K., Kamber, B.S., McGowan, H.A., 2008. Scavenging of atmospheric trace metal pollutants by mineral dusts: inter-regional transport of Australian trace metal pollution to New Zealand. Atmos. Environ. 42, 2460–2478.
Marx, S.K., Rashid, S., Stromsoe, N., 2016. Global-scale patterns in anthropogenic Pb contamination reconstructed from natural archives. Environ. Pollut.
Maussion, F., Scherer, D., Mölg, T., Collier, E., Curio, J., Finkelnburg, R., 2013. Precipitation seasonality and variability over the Tibetan Plateau as resolved by the high Asia reanalysis. J. Clim., 131119065638006
McConnell, J.R., Edwards, R., 2008. Coal burning leaves toxic heavy metal legacy in the Arctic. Proc. Natl. Acad. Sci. U. S. A. 105, 12140–12144.
Merian, E., Anke, M., Ihnat, M., Stoeppler, M., 2004. Elements and Their Compounds in the Environment: Occurrence, Analysis and Biological Relevance. Wiley-VCH Verlag GmbH & Co. KGaA.
Moore, J., Grinsted, A., 2009. Ion fractionation and percolation in ice cores with seasonal melting. Physics of Ice Core Records II, Suppl Issue of Low Temperature Science 68.
Moore, J., Beaudon, E., Kang, S., Divine, D., Isaksson, E., Pohjola, V., Wal, R., 2012. Statistical extraction of volcanic sulphate from nonpolar ice cores. J. Geophys. Res. 117.
Nho, E.-Y., Cloarec, M.-F., Ardouin, B., Tjetjep, W.S., 1996. Source strength assessment of volcanic trace elements emitted from the Indonesian arc. J. Volcanol. Geotherm. Res. 74, 121–129.
Norrish, K., Hutton, J.T., 1969. An accurate X-ray spectrographic method for the analysis of a wide range of geological samples. Geochim. Cosmochim. Acta.
Nriagu, J.O., Pacyna, J.M., 1988. Quantitative assessment of worldwide contamination of air, water and soils by trace metals. Nature 333, 134–139.
Olendrzyński, K., Anderberg, S., Stigliani, W., 1996. Atmospheric emissions and depositions of cadmium, lead, and zinc in Europe during the period 1955–1987. Environ. Rev. 4, 300–320.
Pacyna, J., Pacyna, E., 2001. An assessment of global and regional emissions of trace metals to the atmosphere from anthropogenic sources worldwide. Environ. Rev. 9, 269–298.
Pan, B., Yi, C., Jiang, T., Dong, G., Hu, G., Jin, Y., 2012. Holocene lake-level changes of Linggo Co in central Tibet. Quat. Geochronol. 10, 117–122.
Prakash, P., Stenchikov, G., Tao, W., Yapici, T., Warsama, B., Engelbrecht, J., 2016. Study of Arabian Red Sea coastal soils as potential mineral dust sources. Atmos. Chem. Phys. Discuss. 1–31.
Qian, W., Quan, L., Shi, S., 2002. Variations of the dust storm in China and its climatic control. J. Clim. 15, 1216–1229.
Querol, X., Fernández-Turiel, J.L., López-Soler, A., 1995. Trace elements in coal and their behaviour during combustion in a large power station. Fuel.
Ramanathan, V., Ramana, M., Roberts, G., Kim, D., Corrigan, C., Chung, C., Winker, D., 2007. Warming trends in Asia amplified by brown cloud solar absorption. Nature 448, 575–578.
Reddy, M., Basha, S., Joshi, H.V., Jha, B., 2005. Evaluation of the emission characteristics of trace metals from coal and fuel oil fired power plants and their fate during combustion. J. Hazard. Mater. 123, 242–249.
Rhode, D., Madsen, D.B., Brantingham, P.J., 2007. Yaks, yak dung, and prehistoric human habitation of the Tibetan Plateau. Dev. Quatern Sci. 9, 205–224.
Shao, Y., Dong, C.H., 2006. A review on East Asian dust storm climate, modelling and monitoring. Glob. Planet. Chang. 52, 1–22.
Shaw, D., 1960. The geochemistry of scapolite part II. Trace elements, petrology, and general geochemistry. J. Petrol.
Shaw, D., Reilly, G., Muysson, J., Pattenden, G., Campbell, F., 1967. An estimate of the chemical composition of the Canadian Precambrian shield. Can. J. Earth Sci. 4, 829–853.
Stein, A.F., Draxler, R.R., Rolph, G.D., Stunder, B.J.B., Cohen, M.D., Ngan, F., 2015. NOAA's HYSPLIT atmospheric transport and dispersion modeling system. Bull. Am. Meteor. Soc. 96, 2059–2077.
Streets, D., Shindell, D., Lu, Z., Faluvegi, G., 2013. Radiative forcing due to major aerosol emitting sectors in China and India. Geophys. Res. Lett. 40, 4409–4414.
Swaine, D., 2000. Why trace elements are important. Fuel Process. Technol. 65, 21–33.
Thompson, L., Mosley-Thompson, E., Davis, M.E., Henderson, K.A., Lin, P.-N., 2000. A high-resolution millennial record of the south Asian monsoon from Himalayan ice cores. Science 289, 19161919.
Thompson, L.G., Mosley-Thompson, E., Davis, M.E., Bolzan, J.F., Dai, J., Yao, T., Gundestrup, N., Wu, X., Klein, L., Xie, Z., 1989. Holocene-late Pleistocene climatic ice core records from Qinghai-Tibetan Plateau. Science 246, 474–477.
Thompson, L., Yao, T., Davis, M., Mosley-Thompson, E., Mashiotta, T., Lin, P.-N., Mikhalenko, V., Zagorodnov, V., 2006. Holocene climate variability archived in the Puruogangri ice cap on the central Tibetan Plateau. Ann. Glaciol. 43, 6169.
Tian, L., Yao, T., MacClune, K., White, J., Schilla, A., Vaughn, B., Vachon, R., Ichiyanagi, K., 2007. Stable isotopic variations in west China: a consideration of moisture sources. J. Geophys. Res. Atmos. 112.
Tian, H., Zhao, D., He, M.C., Wang, Y., Cheng, K., 2011. Temporal and spatial distribution of atmospheric antimony emission inventories from coal combustion in China. Environ. Pollut. 159, 1613–1619.
Tian, H., Zhao, D., Cheng, K., Lu, L., He, M., Hao, J., 2012. Anthropogenic atmospheric emissions of antimony and its spatial distribution characteristics in China. Environ. Sci. Technol. 46, 39733980.
Tian, H.Z., Zhu, C.Y., Gao, J.J., Cheng, K., Hao, J.M., Wang, K., Hua, S.B., Wang, Y., Zhou, J.R., 2015. Quantitative assessment of atmospheric emissions of toxic heavy metals from anthropogenic sources in China: historical trend, spatial distribution, uncertainties, and control policies. Atmos. Chem. Phys. 15, 10127–10147.
Uglietti, C., Gabrielli, P., Olesik, J., Lutton, A., Thompson, L., 2014. Large variability of trace element mass fractions determined by ICP-SFMS in ice core samples from worldwide high altitude glaciers. Appl. Geochem. 47, 109–121.
Uglietti, C., Gabrielli, P., Cooke, C., Vallelonga, P., Thompson, L., 2015. Widespread pollution of the South American atmosphere predates the industrial revolution by 240 y. Proc. Natl. Acad. Sci. U. S. A. 112, 2349–2354.
USGS (United States Geological Survey), 1995. The Mineral Industry of Kazakhstan. http://minerals.usgs.gov/minerals/pubs/country/1994/9422094.pdf.

Vejahati, F., Xu, Z., Gupta, R., 2010. Trace elements in coal: associations with coal and minerals and their behavior during coal utilization – a review. Fuel 89, 904–911.
Wang, J., Tomita, A., 2003. A chemistry on the volatility of some trace elements during coal combustion and pyrolysis. Energy Fuel 17, 954–960.
Wang, X., Yang, H., Gong, P., Zhao, X., Wu, G., Turner, S., Yao, T., 2010. One century sedimentary records of polycyclic aromatic hydrocarbons, mercury and trace elements in the Qinghai Lake, Tibetan Plateau. Environ. Pollut. 158, 3065–3070.
Webster, P.J., Magana, V.O., Palmer, T.N., 1998. Monsoons: processes, predictability, and the prospects for prediction. J. Geophys. Res. 103, 14451–14510.
Wedepohl, K., 1995. The composition of the continental crust. Geochim. Cosmochim. Acta 59, 12171232.
Williams, H.M., Turner, S.P., Pearce, J.A., Kelley, S.P., 2004. Nature of the source regions for post-collisional, potassic magmatism in southern and northern Tibet from geochemical variations and inverse trace element modelling. J. Petrol. 45, 555–607.
Wong, G., Hawley, R., Lutz, E., Osterberg, E., 2013. Trace-element and physical response to melt percolation in summit (Greenland) snow. Ann. Glaciol. 54, 52–62.
Wu, G., Zhang, C., Xu, B., Mao, R., Joswiak, D., Wang, N., Yao, T., 2013. Atmospheric dust from a shallow ice core from Tanggula: implications for drought in the central Tibetan Plateau over the past 155 years. Quat. Sci. Rev. 59, 57–66.
Xu, M., Yan, R., Zheng, C., Qiao, Y., Han, J., Sheng, C., 2004. Status of trace element emission in a coal combustion process: a review. Fuel Process. Technol. 85, 215–237.
Xu, J., Grumbine, R., Shrestha, A., Eriksson, M., Yang, X., Wang, Y., Wilkes, A., 2009. The melting Himalayas: cascading effects of climate change on water, biodiversity, and livelihoods. Conserv. Biol. 23, 520–530.
Yan, L., Zheng, M., 2015. Influence of climate change on saline lakes of the Tibet Plateau, 1973–2010. Geomorphology 246, 68–78.
Yan, R., Gauthier, D., Flamant, G., 2001. Volatility and chemistry of trace elements in a coal combustor. Fuel 80, 2217–2226.
Yanai, M., Li, C., Song, Z., 1992. Seasonal heating of the Tibetan Plateau and its effects on the evolution of the Asian summer monsoon. J. Meteorol. Soc. Jpn.
Yang, B., 2004. Horses, silver, and cowries: Yunnan in global perspective. J. World Hist.
Yang, B., Bräuning, A., Zhang, Z., Dong, Z., Esper, J., 2007. Dust storm frequency and its relation to climate changes in Northern China during the past 1000 years. Atmos. Environ. 41, 9288–9299.
Yang, X., Yao, T., Joswiak, D., Yao, P., 2014. Integration of Tibetan Plateau ice-core temperature records and the influence of atmospheric circulation on isotopic signals in the past century. Quat. Res. 81, 520–530.
Yang, Y., Fang, X., Galy, A., Zhang, G., Liu, S., Zan, J., et al., 2015. Carbonate composition and its impact on fluvial geochemistry in the NE Tibetan Plateau region. Chem. Geol. 410, 138–148.
Yang, S., Ding, Z., Li, Y., Wang, X., Jiang, W., Huang, X., 2016. Reply to Yu et al.: global temperature change as the ultimate driver of the shift in the summer monsoon rain belt in East Asia. Proc. Natl. Acad. Sci. 113, E2211–E2212.
Yao, T., Shi, Y., Thompson, L.G., 1997. High resolution record of paleoclimate since the Little Ice Age from the Tibetan ice cores. Quat. Int. 37, 19–23.
Yao, T., Duan, K., Xu, B., Wang, N., Guo, X., Yang, X., 2008. Precipitation record since AD 1600 from ice cores on the central Tibetan Plateau. Clim. Past 4, 175–180.
Yao, T., Thompson, L., Yang, W., Yu, W., Gao, Y., Guo, X., et al., 2012. Different glacier status with atmospheric circulations in Tibetan Plateau and surroundings. Nat. Clim. Chang. 2, 663–667.
Yao, T., Masson-Delmotte, V., Gao, J., Yu, W., Yang, X., Risi, C., et al., 2013. A review of climatic controls on $\delta^{18}O$ in precipitation over the Tibetan Plateau: observations and simulations. Rev. Geophys. 51, 525–548.
You, Q., Kang, S., Aguilar, E., Yan, Y., 2008. Changes in daily climate extremes in the eastern and central Tibetan Plateau during 1961–2005. J. Geophys. Res. Atmos. 113 (1984–2012).
Yu, S., Li, P., Wang, L., Wang, P., Wang, S., Chang, S., Liu, W., Alapaty, K., 2016. Anthropogenic aerosols are a potential cause for migration of the summer monsoon rain belt in China. Proc. Natl. Acad. Sci. 113, E2209–E2210.
Zhang, B., 2014. The basic study of the Cs-bearing geyserite deposit in Targejia, Tibet. Acta Geologica Sinica Engl. Ed. 88, 942–943.
Zhang, X., Arimoto, R., Cao, J., An, Z., Wang, D., 2001. Atmospheric dust aerosol over the Tibetan Plateau. J. Geophys. Res. Atmos. 106, 18471–18476.
Zhang, Q., Kang, S., Kaspari, S., Li, C., Qin, D., Mayewski, P., Hou, S., 2009. Rare earth elements in an ice core from Mt. Everest: seasonal variations and potential sources. Atmos. Res. 94, 300–312.
Zhang, X., Wang, J., Wang, Y., Liu, H., Sun, J., Zhang, Y., 2015. Changes in chemical components of aerosol particles in different haze regions in China from 2006 to 2013 and contribution of meteorological factors. Atmos. Chem. Phys. 15, 12935–12952.
Zheng, M., Liu, X., 2009. Hydrochemistry of Salt Lakes of the Qinghai-Tibet Plateau, China. Aquat. Geochem. 15, 293–320.
Zhou, Y., Xing, X., Lang, J., Chen, D., Cheng, S., Wei, L., 2017. A comprehensive biomass burning emission inventory with high spatial and temporal resolution in China. Atmos. Chem. Phys. 17, 2839–2864.
Zoller, W.H., Gladney, E.S., Duce, R.A., 1974. Atmospheric concentrations and sources of trace metals at the South Pole. Science 183, 198–200.